Hydrodynamic Analysis of Different Textured Profile Thrust Bearing

A Thesis Submitted in Partial Fulfillment of the Requirements for the

Award of the Degree of

Master of Technology
in
Mechanical Engineering

(Machine Design & Analysis)

By

Durjyodhan Sethi

Roll No.212ME1281

Under the Supervision of

Prof. Suraj Kumar Behera

NATIONAL INSTITUTE OF TECHNOLOGY ROURKELA

राष्ट्रीय प्रौधोगिकी संस्थान राउरकेऱा

ROURKELA 769008
ODISHA, INDIA

June 2014

National Institute of Technology Rourkela

Certificate

This is to certify that the thesis entitled, "**Hydrodynamic Analysis of Different Textured Profile Thrust Bearing**" submitted by Mr**. Durjyodhan Sethi** to National Institute of Technology Rourkela, during the academic session 2012-2014 is a record of bonafide research work carried out by him under my supervision and is worthy of consideration for the award of the degree of Masters of Technology in Mechanical Engineering with specialization in **Machine Design and Analysis.** The embodiment of this thesis has not been submitted to any Other University and/or Institute for the award of any degree or diploma.

Date: 2nd Jun, 2014

Prof. Suraj Kumar Behera
Dept. of Mechanical Engineering
National Institute of Technology
Rourkela-769008

DEPARTMENT OF MECHANICAL ENGINEERING
NATIONAL INSTITUTE OF TECHNOLOGY
ROURKELA 769008

ACKNOWLEDGEMENT

It gives me immense pleasure to express my deep sense of gratitude to my supervisor **Prof. Suraj Kumar Behera** for her invaluable guidance, motivation, constant inspiration and above all for her ever co-operating attitude that enabled me in bringing up this thesis in the present form.

I am thankful to **Prof. K. P. Maity**, Head, Department of Mechanical Engineering for providing all kinds of possible help and advice during the Course of this work.

I would like to thank Mr. Ranjan kumar Behera M.Tech scholar, Department of Mechanical Engineering for his valuable suggestion during the research work. I am greatly thankful to all the staff members of the department and all my well-wishers, class mates and friends for their inspiration and help.

I would like to thanks my parents for their unconditional support, love and affection. Their encouragement and never ending kindness made everything easier to achieve.

Abstract

Surface texture in the surface of the thrust bearing reduces the friction coefficient and wear rate of the matting surface. Significant improvement in load carrying capacity, wear resistance and friction coefficient of the tribiological mechanical component can be achieved by forming regular micro structure in form of micro dimple on the thrust pad bearing surface. In the present work numerical analysis is carried out to investigate the effect of spherical, cylindrical, elliptical, rectangular and square texture on the thrust pad hydrodynamic bearing and a comparison is done with the plain thrust bearing. The above texture profile was chosen in the view to easy fabrication of such texture using laser technology or etching process**.** These textured pads are tested on the various type of operating condition. The Reynolds equations are solved numerically by the finite difference method and an analysis is done on the effect of texture height, aspect ratio, and number of textures both in radial and circumferential directions on thrust pad bearing. It is observed that the load carrying capacity increases with increase of texture height ratio. This is because as texture height is increased it restricts the flow of lubricants which increases pressure and load carrying capacity. The analysis shows as aspect ratio is increased the roughness of surface is increased so pressure is increased, which result is increasing load carrying capacity. However with very larger value of aspect ratio the roughness of surface decreases, which decreases the load carrying capacity. Similar studies the done for behavior of coefficient of friction on variation of aspect ratio, texture height ratio etc. The author believes that such detail analysis on different texture profile on thrust pad hydrodynamic to study different tribological behavior under different condition will help researchers around the world.

CONTENTS

TITLE **PAGE.NO**

LIST OF TABLE

LIST OF FIGURES

Nomenclatures:

U_r, U_θ, U_z : Velocity components in r, θ, z directions respectively (m/s)

ρ: Density of lubricant (Kg/m^3)

η: Dynamic viscosity of lubricant ($N\text{-}sec/m^2$)

h : Lubricant film thickness (mm)

$\bar{h}$ **:** Non-dimensional film thickness

C : Clearance (mm)

C_g: Texture height (mm)

$\overline{Cg}$**:** Non-dimensional texture height

r_i : Inner radius of thrust pad (mm)

r_o: Outer radius of thrust pad (mm)

$\bar{\theta}$ **,**$\bar{Z}$**:** Non-dimensional co-ordinates

$\bar{W}$ **:** Non-dimensional load

$\bar{Q}$**:** Non-dimensional flow

$\bar{F}$ **:** Non-dimensional frictional force

$\bar{f}$**:** Non-dimensional co-efficient of friction

$\bar{p}$: Non-dimensional pressure

THR: Texture height ratio

AR: Aspect ratio

CHAPTER 1

1. INTRODUCTION

1.1 Background

Tribology is defined study of friction, lubrication, wear and contact mechanics of engineering surface. Tribology has a significant impact on economic like maintenance, reliability and wear between the equipment starting from house hold appliances to spacecraft. Successful design of mechanical machine element with relative motion depends up on the understanding of tribological behavior of mating surfaces, so tribology is vital in the modern machinery. In modern machinery design of bearings (both radial and axial) for rotors plays an important role as due to requirements of mankind. The size, speed and load of rotor are changing, so different types of bearings are necessary to satisfy the need of engineering society.

The load carrying capacity of journal (radial) and thrust (axial) bearings depends on many factors; among them wedging action contribute significantly for pressure development. For a horizontal rotor wedging action in journal bearings comes into picture by virtue of gravitational pull of rotor. However in thrust bearing geometry modification is required for wedging action. In current investigation an effort is given to find different frictional parameters by modifying geometry of thrust bearing surface.

In the field of Tribology, to reduce friction at every level of technology efforts have been there. Micro fabrication techniques along with development in microscopy (optical, scanning electrons and atomic force microscopes) has implemented in tribological applications at microscopic level. With the help of advanced technology positive and negative microstructures are possible on thrust bearing surfaces, face seal etc. Due to the presence of micro structures tribological performance (friction, wear, interfacial temp, and life time) is enhanced. Engineered surfaces are found to be beneficial in many contact applications with or without the presence of any lubricant. So in current analysis the thrust bearing surface are provided with different texture profile to enhance tribological performance.

1.2 Thesis overview

Creating surface texture in form of micro-scale asperities on mechanical component surface produce unequal pressure distribution as a results hydrodynamic lift can take place. Micro asperities are micro and nano sized peaks and valleys that form surface roughness. Depending on shape, size and orientation of micro asperities, surface textures enhance the hydrodynamic effects on thrust bearing. The theoretical analysis is carried out in hydrodynamic thrust bearing with engineered texture profile like spherical, cylindrical, elliptical, rectangular and square to find the importance of tribological parameters such as co-efficient of friction, load carrying capacity for different aspect ratio and texture height ratio.

1.3 Objectives of the Present Work

Current work aimed to study the hydrodynamic thrust pad bearing with positive and negative micro textures. Followings are the main objectives of present work.

1. Development of a numerical solution to investigate the effect of positive and negative spherical, elliptical, cylindrical, square and rectangle shape micro textures on thrust pad bearing.
2. Analysis is done varying three parameters namely aspect ratio, texture height ratio and number of textures both in radial and circumferential directions.
3. Validation of numerical solution for the case of plain thrust pad bearing with the previously available results.
4. Finally comparison of tribological parameters has been plotted for different textured profile.

1.4 Basic concepts

1.4.1 Surface topography

Tribological phenomenon occurs on the mating surfaces, so the surface structure variation is the key point to the study the mechanism of friction and wear. Surface imperfections at an atomic level are matched by macroscopic deviations from flatness. Almost all surfaces except cleaved faces of mica are rough. Roughness means most parts of surfaces from peaks and valleys. The profile of rough surface is almost always random unless some regular features have been deliberatively introduced. The unique property of surface roughness is that, if repeatedly

magnified, increasing the details of surface features are observed down to the Nano scales.

Most real engineering surfaces consists of a blend of random and nonrandom features. The series of grooves formed by a shaper on a metal surface are prime example of nonrandom topological characteristics. Bead blasted surfaces consist almost entirely of random features, because of random nature of this process. The shaped surfaces also contain high degree of random surface features which gives its rough texture. On random features do not significantly affect the contact area and contact stress provided that random roughness is superimposed on nonrandom features.

Contact between solid surfaces is discrete (discontinuous) due to deviations of surface geometry from design shape (macro geometry). So real contact region consists of contact spots, the total area (real contact area) is a small fraction of nominal contact area which is the minimal connected region enclosing all contact spots. The size and arrangement of contact spots depend on contact interaction conditions (load, kind of motion etc.), materials, surface macro geometry and deviations from it.

These deviations (asperities) have various sizes and shapes. Their heights vary within wide limits: from fraction of a nanometer to several millimeters. Depending on the scale, they are called macro deviations, waviness or roughness. Macro deviations are characterized by small height and asperities with gentle slopes. For waviness the ratio of distance between asperities to asperity height is more than 40. Roughness is the conglomeration of asperities with small pitch relative to base length.

Micro geometry of surface can also be created artificially to provide optimal conditions for frictional components to operate .Surfaces with artificial micro geometry are widely applied in devices used for processing and storing information. Profilometers, optical interferometers, tunnel and atomic pound microscopes are used to describe the micro geometry of a given element of surface and to determine its surface characteristics such as mean height, mean curvature of asperities, number of asperities per unit area of surface.

1.4.2 Friction

According to modern conception of tribology there are two main causes of energy dissipation which gives rise to resistances in sliding contact. The first one associated with work done in

making and breaking adhesion bonds formed in the points of contact of sliding surfaces. The force necessary to shear these bonds is termed the adhesive (molecular) component of friction force. The mechanism for formation of adhesion bonds depend on the properties of the contacting bodies. A third body is a thin layer at the interface between contacting bodies. Its properties depend on mechanical properties of the surface layers of contacting bodies, boundary film etc.

The second cause of energy dissipation is cycle deformation of bodies in sliding contact. The resistive force connected with this process is termed as mechanical component of friction. It depends on mechanical properties of bodies, geometry of their surfaces, applied forces etc. The mechanical component of friction force depends on deformation of bodies in contact. The relation between components of friction force depends on friction condition, mechanical properties of contacting bodies. Energy dissipation also occurs in rolling contact. The resistive to rolling is caused by the followings:

1. Friction due relative slip of surfaces within the contact area rising from differences of curvature of contacting surfaces and different mechanical properties.
2. Imperfect elasticity of contacting bodies.
3. The adhesive forces in contact.

1.4.3 Wear

Wear may be defined as progressive loss of substance from the operating surface of a body occurring as a result of relative motion at the surface. Most tribological pairs are supplied with lubricant as much to avoid excessive wear and damage which would present if two surfaces are allowed to rub together dry as it as to reduce their frictional resistance to motion. The economic consequences of wear are widespread. They involve not only cost of replacement of parts but also expenses involved in machine downtime, loss of production. The wear rate of rolling or sliding contact is conventionally defined as the volume lost from wearing surface per sliding distances. For particular dry or unlubricated sliding situation the wear rate depends on normal load, relative sliding speed, initial temperature and thermal, mechanical and chemical properties of the materials in contact.

1.4.4 Lubrication

Thin low shear strength layers of gas, liquid and solid are interposed between two surfaces in order to improve the smoothness of movement of one surface over another and to prevent damage. These layers of material separate contacting solid bodies and are usually very thin (1-100μm) and to prevent damage. The effectiveness of these films in preventing damage in solid contact is commonly known as 'lubrication'. Analysis of gaseous or liquid films is termed as 'hydrodynamic lubrication'. A hydrodynamic lubrication involving physical interaction between the contacting bodies and liquid lubricant is termed as 'elasto-hydrodynamic lubrication'.

1.5 Fluid Film Lubrication

A bearing is a device which permits two components in a mechanism to move relative to one another in either one or two dimensional while constraining their movement in the remaining dimension. The simplest arrangement which while supporting substantial normal loads allows motion in one direction only is linear bearing, more common engineering use than this is journal bearing which permits a cylindrical shaft, the journal to rotate while carrying a radial load. In order to reduce frictional resistance, wear and carry away heat generated, a layer of lubricant is used in the clearance space.

Bearings are classified according to the direction of applied load. If the bearing supports a radial load it is called radial or journal bearing. If bearing support axial load, it is called thrust bearing. Bearings can be broadly classified as fluid film bearing and rolling element bearing. If mating surfaces are separated by lubricant film, these types of bearings are called fluid film bearing. Fluid film bearings are two types:

1 Self-acting / hydrodynamic bearing
2 Externally pressurized / hydrostatic bearing

In hydrodynamic lubrication, the pressure is generated by relative movement of mating surfaces. In hydrodynamic bearing the film breaks down during starting and stopping of the machine. All self-acting hydrodynamic bearings depend for their successful operation on the presence of converging, wedge shaped gap into which the viscous fluid is dragged by relative motion of solids. A pressure is generated which leads to push the faces of wedge apart and it is the

integrated effect of this pressure distribution within fluid that balances the normal load on the bearing.

1.6 Surface Textures

A surface, by definition is an interface, a marked discontinuity from one material to another. Any real surface has a finite depth and in characterizing a surface one must at some point consider what this depth is. The texture of any surface is defined by the inherent surface topography it exhibits. All surfaces have a unique texture and structure and all manufactured surfaces are 'engineered'. Design engineers have an understanding of the relationship between surface texture and its function. Textured surfaces create a lubrication film, which produces a load carrying capacity when there is no condition for the wedge effect. The idea appeared by observing an optimal roughness, which leads to local load carrying capacity effects.

1.6.1 Deterministic Asperities

Micro asperities are the micro and Nano sized peaks and valleys on a surface that constitute surface roughness. Deterministic micro asperities are the asperities of prescribed shape, size, orientation distribution that comprise an engineered surface texture. Macro asperities are typically large area surface features with extremely low height to diameter (aspect ratio) <0.0001. Macro surface features are typically few in number and can be manufactured with comparative ease using processes including grinding and chemical etching. On the other hand deterministic micro asperities are orders of magnitude smaller in average diameter, significantly greater in number and larger aspect ratio. Methods to fabricate such asperities traditionally include photo etching, laser texturing, LIGA process (German acronym for lithography, electroplating & molding) & UV photo lithography process. Modified LIGA process which basically well known as LIGA process with UV light as a substitute for X-ray. The concept of surface texturing was developed after 1990 using primarily laser technology. Surface texturing found a large number of industrial applications. In case of mechanical seals this technology enhances axial stiffness. Load carrying capacity is created in fluid film of a couple having one textured surface even if two mating surfaces are parallel. Surface texturing has proved to be very efficient in full and mixed lubrication, reducing friction coefficient, wear rate, increase load capacity, dynamic stiffness and damping coefficient.

Positive Asperities

These are micron scaled surface featured of any arbitrary geometry that is in the form of protrusion on a surface. The protrusions (bumps, posts) are called positive asperities. Figure 1.1 and figure 1.2 shows the positive asperities.

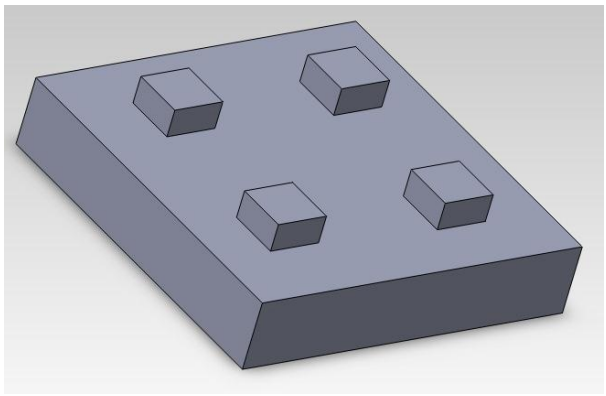

Fig 1.1: Square Positive Asperity

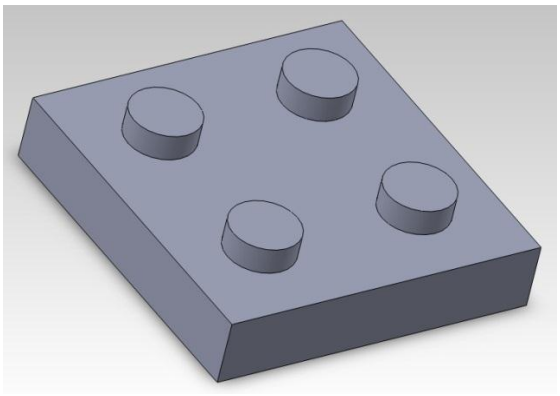

Fig 1.2: Cylindrical Positive Asperity

Negative asperities

These are micron scaled surface features of any arbitrary geometry that are in the form of cavities on a surface. Recesses (holes) are called negative asperities. Figure 1.3 and figure 1.4 shows the negative asperities.

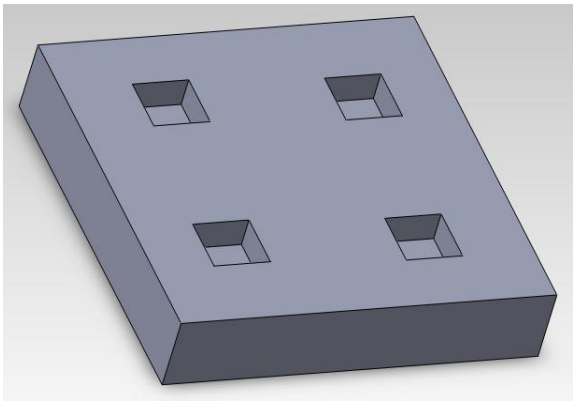

Fig 1.3: Square Negative Asperity

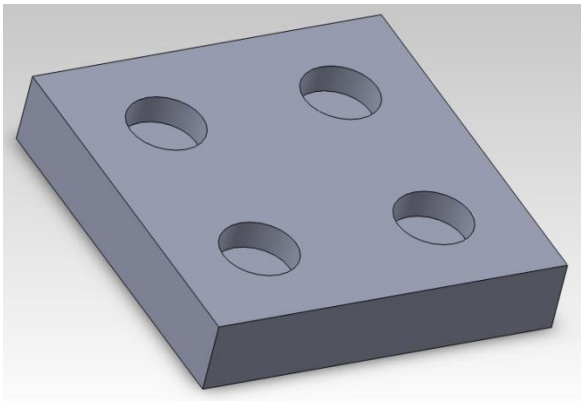

Fig 1.4: Cylindrical Negative Asperity

a. LIGA can produce either positive (protuberances) or negative (recesses) asperities of any cross section.
b.Laser texturing method can produce only negative asperities of spherical or conical geometry.

CHAPTER 2

2. Literature Survey

Although a considerable amount work has been reported on the study of surface texture on hydrodynamic thrust bearing. This chapter is intend for reporting list of several work on the texture profile thrust bearing and understanding various aspect of the surface texture thrust bearing and study the performance parameter

Surface texturing is a method for improving tribological properties of of mechanical component for many years. Introducing surface texture to one of two faces in relative motion can have improve tribological property, like reduction of coefficient of friction parameter and wear rate and increase in load capacity of the bearing.The surface texture in form of of micro asperities act as microhydrodynamic bearing which lift the load during film lubrication

Micro-texture consists of micron-scale surface features such as positive or negative texture profile. Initial the textures size were limited to grooves and troughs, later with help of advance technology various type of complex patterns of different shapes and size including circular, triangular, elliptical, square, rectangle are used. Asperity Aspect Ratio, texture height, area, depth and orientation are impact the effectiveness of a given texture

Various types of the methods are used for creating this surface texture. Photo etching, laser texturing, LIGA process & UV photo lithography process. Modified LIGA process which basically well known as LIGA process with UV light as a substitute for X-ray .Mechanical techniques like viborolling and abrasive machining can also be used to create grooves. For metal and ceramic etching and lithography are used for producing variety of shapes micro structure. Presently laser surface texturing (LST) used for a versatile and high-speed texturing method .

Recent and past studies have study the effects of these different methods and of various micro asperity parameters on Coefficient of friction, wear, and load carrying capacity.

Sadeghi et al [1] study the use of micro pores which is used as lubricant for a highly-loaded case .In the experiment he has shown that during start up and shut down time load is lifted due to both solid and lubricant .there is reduction in friction when the surface pocket are introduce.The

volume of the pocket decrease when the load acted upon the pocket due to compression of the pocket take places. Due to compression it help lubricant to support the load and reduce the friction.

Surface textures is one of best method which is used for designing in the mechanical seal . hydrodynamic lift in the bearing can be created with help of producing macro-scale on their surface as result load-carrying capacity of the bearing seal increase .Due to micro-scale texturing it provide additional hydrodynamic lift, this is not used in full-surface texture case but some areas where we create virtual macro scale surface structure.

Tonder et al [2] In his analytically observation conclude that, for creating hydrodynamic pressure in between two sliding seal a region of micro texturing can replace by another macro-feature . The main purpose of producing micro texture is decrease the area the flow of lubrication in the seal so that it resists the flow of lubrication during the fluid travels through the seal as result hydrodynamic pressure is generated in the bearing. From the Analytical results it conclude that a grooved entry area have lower friction coefficient and leakage than that generally used macro-feature such as the region which are inclined. Surface which have round and square dimples have benefit then other shape. Higher damping in the textured surfaces over the un texture surface .Small amplitude of vibration can be achieved in the case of thin-film seals with the thinner the film

The hydrodynamic theory of lubrication stems out directly from the experiments of Tower [3] in1883.During his experiments on rails road axles that a hydrodynamic pressure was developed in the bearings. In the same year Petroff [4] attempted to analyze theoretically the viscous friction effect of film lubrication. Both Tower & Petroff however failed to provide theoretical basis of their experimental results. This was achieved by Reynold [5] in1886.Reynold could derive the differential equation in pressure for a thin oil film between two moving surfaces.

Producing texturing in the surface considered as feasible method for improving the tribological properties of surface from 1965. By putting deterministic asperities (both positive and negative asperities) to one of two moving surfaces can have positive effects, it reduce of friction coefficient, wear and increase the load carrying capacity of the bearing**.**

Early studies the benefits of micro asperities to provide hydrodynamic lift in the bearing during film lubrication [6], while research conclude that micro textured surfaces act as reservoirs in boundary and dry lubrication. In these work the authors experimentally investigated three samples consisting of circular or square shaped asperities distributed in a hexagonal or square array. From this work the authors concluded that (a) Hydrodynamic performance is largely insensitive to asperity shape. (b)Negative asperity patters results in less leakage.

In 1996 Etsion and Burstein examined hemispherical pores on square array on one of the mating seal face. The authors found that asperity size significantly affects friction, leakage and film thickness. The micro textured surfaces may be used further for partial texturing,a textured region can act as steps or squeeze film and inclined planes means to provide hydrodynamic wedge action [7].All have effect to decrease the friction coefficient and wear between two parallel sliding surfaces. Research and analysis presented to improve tribological properties through surface texturing. Micro topography consists of micron scaled surface features of positive (protruding) or negative (cut) surfaces

Marian Victor [8] study that when there is no wedge action initial, creating texture shape on the surfaces of the bearing, a lubrication film is produces as a result load carrying capacity increase. This phenomenon of creating texture shape large widely used in various industrial applications like improving the mechanical seals in the bearing, manufacturing of partial textured thrust pad bearings, it can be used in the internal combustion engine for reducing fuel consumption rate by creating texture in the piston ring also due to texturing durability of the cylindrical roller bearing increases. The pressure distribution in the textured surface of all the application can be calculated by finite difference method.

Mircea D. Pascovici et al [9] presented analytical & numerical analysis of partial textured slider bearing. In this approach the pressure distribution in the bearing is calculated with help of above two methods and the performance of the bearing is calculated. Bearing performance evaluated by various parameters like number of dimples in the bearing, texture density in the bearing, dimple

depth and textured fraction of the slide bearings. The optimal value for the slider bearing is determined for maximum pressure and maximum load carrying capacity of the bearing. The authors found that partially textured structure bearing has lower load carrying capacity than the stepped slider bearing, but partial structure can be easily manufactured with help of various technologies.

V G Marian et al. [10] published a paper, in which a partially surface texture in the thrust bearing with the square dimples shape is analyzed theoretically with help of thermo hydrodynamic model. In the photolithographic method theoretical results were compared with the experimental result obtained on the test rig. From the observation it concludes that maximum load carrying capacity obtained with textured fraction is 0.5 on the circumferential direction and texture fraction 0.9-1 on the radial direction.

N Tata-Ighil et al. [11] study the effects of texture surface distribution in the contact surface of the bearing. From the investigation it conclude that spherical dimple structure have minimum film thickness, oil flow in the axial direction and with proper surface geometry frictional torque can be increase in the bearing

Haiwu Yu et al [12] analyzed that surface textures in the contact interfaces affect the tribological performance. Producing various type textures shape and different orientations develop the hydrodynamic pressure on hydrodynamic lubrication, Triangle, circle & ellipse textures are taken for produce the hydrodynamic pressure perpendicular to the sliding direction and it shows the hydrodynamic bearing load carrying capacity.

The hydrostatics thrust bearing [13] have low running friction coefficient, high load carrying capacity and high stiffness. These characteristics are observed when we compare with plane thrust bearing .Further the effect of the dynamic stiffness and damping characteristics of the hydrostatics step thrust pad bearing with capillary-compensated is observed .The bearing surface with circumferential roughness have very less influence on the load carrying capacity but it effect on lubrication flow rate, dynamic stiffness and damping coefficient. The arrangement of circumferential roughness in the thrust bearing reduces the dynamic stiffness and damping coefficient but the bearing with fixed radius ratio, the roughness effect in the radial structure

characteristics is reversed. With the low value of the speed number and high value of squeeze number surface roughness effect in dynamic stiffness is more.

Xiaolei wang et al[14]study the effect of SiC thrust bearing in water lubrication, Load carrying capacity increase due to tribo-chemical reaction of SiC with water ,these reaction produce SiO_2 which dissolves in water as a silicic acid and which act as lubricant so the contact surface become very smooth , improving the load carrying capacity in the bearing is still an important research when two parallel surface having surface roughness and waviness of internal parallel surface slide to each other in presence of liquid due to various mechanism the hydrodynamic pressure is generated. Load carrying capacity of SiC thrust bearing with water lubrication increase due micro pit are introduce on one of the contact surface by reacting ion etching that depending up on the geometry and distribution of the micro pit, due to this load carrying capacity increase up to 2.5 time over that un texture surface

T.S Lung et al [15] studied the effect of the porous material as a restrictor in the aerostatic thrust bearing, due to porous material load carrying capacity and stiffness of the bearing increase. Yuntang li, Han Ding study the performance of aerostatic bearing change with different geometrical parameter, in aerostatic thrust pad bearing with pocket type orifice restrictor with small film thickness; small orifice diameter and big air chamber diameter have good performance. the bearing is unstable when depth and diameter of air chamber are ten time and five time of of the minimum value with the restrictor pocket-orifice type. When the length of orifice is not considered, decrease with orifice diameter the performance is large error.

Mohamed fourka et al [16] studied the effect of externally pressurized gas bearing with high bearing stiffness, high damping coefficient and the effect of these properties on the type of feeding. There are two types of orifice first pocketed orifice and second inherent type orifice. In the pocket type orifice bearing have, low damping and poor stability and high stiffness while inherent type exhibit better stability, relatively high damping and low stiffness

The load carrying capacity and stability of porous wall bearing have high but stiffness half that of pocket bearing increase and decrease the stiffness depend the permeability, if the permeability is less than 10^{-12} m^2 then the stiffness of the bearing increase

A.K Mishra [17] Observed that in an aerostatic rectangular thrust pad bearing with off-set load for the constant value of supply pressure with feeding parameter and restrictor parameter, the stability decrease with increase in the pad shape ratio and at the lower pad shape ratio, the bearing is more stable. The stability also decrease with increase in feeding parameter when the other design variable kept constant, it also observed that when gas pressure supply increase the stability of the gas bearing decrease and there is decrease the stability of the bearing with increase of the attitudes of the tilt

M.F Chen et al [18] Aerostatic bearing have low friction losses and low heat generation, with introducing horizontal and vertical it seen that load carrying capacity increase .They investigated the statics characteristics of the aerostatic bearing with X shaped grooves .the groove can done by resistance network method and it is seen that groove bearing provide greater stiffness and load carrying capacity but cause pneumatic hammer with too large width or depth. Using modified resistance network method we calculate impulse response and stability range of the grooved aerostatic bearing and X shaped aerostatic bearing there are decrease stability with decrease groove width and depth. The stability of bearing decrease with increase equilibrium position and increase with increase with increase the dimension size

I.Etsion [19] observe that the improvement of load carrying capacity, friction coefficient and wear resistance of the tribological component can be improved by micro-surface texture in form of micro dimple on their surface by the help of Laser surface texturing. Laser texturing is most promising concept because laser is clean to environment, extremely fast and provide excellent control of the size and shape of the micro dimple, laser surface texture increase the tribological mechanical performance at the same time it also used as a mechanical seal

Xiaolei Wang et al[20] tribological performance of the sliding surface can be improved by surface texturing which created wedge action and it is help for generate hydrodynamic pressure as a result load carrying capacity increase. Silicon carbide slide identical material in water tribo-chemical reaction occur due to these tribo-chemial reaction load carrying capacity increase

The micro-dimples or microgroove are designed in such manner so that they are evenly distributed evenly on the surface. The area ratio and dimension of the texture is considered the important parameter for generation of hydrodynamic pressure

The Due to the surface texture hydrodynamic pressure is generated and improves the load carrying capacity, the running in process of silicon carbide sliding in water, the texture pattern combined with a large dimple and small dimple to improve the load carrying capacity bearing of SiC sliding in water. It is observed that the pattern are mixed with large dimple and small dimple have higher critical load over the small or large dimple

WU Ding -Zhu[21] the porous aerostatic thrust bearing have better load carrying capacity, high stiffness and damping performance characteristics, Permeability of porous media and supply of gas pressure can influence the static performance in load carrying capacity. Stiffness of the bearing increases with increase the supply gas pressure. Thicknesses of porous media and restrictor working face have great impact on statics performance in both load carrying capacity and static stiffness

A.Shinkarenko et al [22] study the effect of the surface texturing on soft elasto-hydrodynamic with the axial relative motion in rod seal texturing in the form of spherical micro dimple was applied in rigid surface and soft elastomer surface. It was found that provide texture on the surface load carrying capacity can be achieve maximum value with some optimum texturing parameter like dimple aspect ratio and area density

Surface texturing is advance technology which is used to generate hydrodynamic pressure between two normally parallel surfaces that move relative to each other with Newtonian laminar flow. surface texturing also provide hydraulic seal .different form of surface texturing like wave ,asperities, dimple are created on the bearing surface for increase load carrying capacity and hydraulic seal

Mohamed Fourk et al [23] studied the stability of air thrust pad bearing of a non-linear model which is based up on finite element method. In the high precision machine there is need to achieve high stiffness and high damping .The mechanism of stability range of circular thrust bearing has been calculated and the numerically resulted were compared with analytical

prediction and experiment result. From the experiment it is seen that the pocket and orifice groove compensation geometry have influence the stability of air thrust bearing

Y.K .Younes [24] studies the effect of surface irregularities, surface waviness and surface roughness in bearing and their performance with the lubricated bearing. In the rotating hydrostatic thrust pad circular bearing with smooth and parallel sill and flat surface, It seen that in absence of any wedge action, there is no hydrodynamic pressure is generated .in the hydrostatic thrust bearing presence of sill in form of undulation shaped on their surface, in presence of undulation a wedge action is created in which the direction the bearing slide as result hydrodynamic pressure is created and the load carrying capacity of that bearing increase

S.N Rao [25] study the static characteristic of aero static thrust bearing with rectangular structure porous which is uniformly is present on the surface. it is seen that load carrying capacity of the bearing, static stiffness and mass flow are reduces due to velocity slip . At the surface boundary condition are assumed conventional and adherence with non-zero tangential velocity and this velocity know as slip velocity at the permeable surface. The effect of slip flow on the static characteristic with the feeding parameter, pad ratio and supply pressure is compare with the circular thrust bearing for the boundary condition with no slip

CHAPTER 3

3. Theoretical and Numerical Analysis

The generalized lubrication theory is based up on the particular form of Navier-Stokes equations. The basic Reynolds equation is a differential form equation which is combination of Navier-stokes and continuity equation containing pressure which is frequently used in the hydrodynamic lubrication theory under some assumptions. In Reynolds equation the parameter contain lubricant viscosity, density and film thickness of lubricant. From the Reynolds equation, the energy equation and the equation of state, accurate hydrodynamics fluid film can be obtained.

3.1 Governing Equation

The continuity equation and momentum equation are sufficient to describe lubrication flows for Newtonian fluids; combination of two is called Reynolds equation. To attain this form of continuity equation and equation of motion, first step is to assume lubrication approximation which relates the relative importance of the distance in the sliding direction and film thickness. The generalized Navier-Stroke equation in cylindrical coordinate system (i.e. r, θ, z) for thrust bearing is given by equation 3.1, 3.2 and 3.3:

$$\rho\left(\frac{\partial U_r}{\partial t}+U_r\frac{\partial U_r}{\partial r}+\frac{U_\theta}{r}\frac{\partial U_r}{\partial \theta}+U_z\frac{U_r}{\partial z}-\frac{{U_\theta}^2}{r}\right)$$

$$=-\frac{\partial p}{\partial r}+\eta\left[\frac{1}{r}\frac{\partial}{\partial r}\left(r\frac{\partial U_r}{\partial r}\right)+\frac{1}{r^2}\frac{\partial^2 U_r}{\partial \theta^2}+\frac{\partial^2 U_r}{\partial Z^2}-\frac{U_r}{r^2}-\frac{2}{r^2}\frac{\partial U_\theta}{\partial \theta}\right]+\rho g_r \qquad 3.1$$

$$\rho\left(\frac{\partial U_\theta}{\partial t}+U_\theta\frac{\partial U_\theta}{\partial r}+\frac{U_\theta}{r}\frac{\partial U_\theta}{\partial \theta}+U_z\frac{\partial U_\theta}{\partial z}+\frac{U_r U_\theta}{r}\right)$$

$$=-\frac{1}{r}\frac{\partial p}{\partial r}+\eta\left[\frac{1}{r}\frac{\partial}{\partial r}\left(r\frac{\partial U_\theta}{\partial \theta}\right)+\frac{1}{r^2}\frac{\partial^2 U_\theta}{\partial \theta^2}+\frac{\partial^2 U_\theta}{\partial z^2}-\frac{U_\theta}{r^2}+\frac{2}{r^2}\frac{\partial U_r}{\partial \theta}\right]+\rho g_\theta \qquad 3.2$$

$$\rho\left(\frac{\partial U_z}{\partial t}+U_r\frac{\partial U_z}{\partial r}+\frac{U_\theta}{r}\frac{\partial U_z}{\partial r}+U_z\frac{\partial U_z}{\partial z}\right)$$

$$=-\frac{\partial p}{\partial z}+\eta\left[\frac{1}{r}\frac{\partial}{\partial r}\left(r\frac{\partial U_z}{\partial r}\right)+\frac{1}{r^2}\frac{\partial^2 U_z}{\partial\theta^2}+\frac{\partial^2 U_z}{\partial z^2}\right]+\rho g_z \qquad 3.3$$

In the above equation (3.1), (3.2) and (3.3) ,there is gravity components, which are not constant but for most of application the co-ordinate chosen so that gravity component are constant. Generally it is assumed that gravity component is compensated by pressure field.

The continuity equation in the polar co-ordinate(r,θ,z) is given in equation 3.4.

$$\frac{\partial\rho}{\partial t}+\frac{1}{r}\frac{\partial}{\partial r}(\rho r U_r)+\frac{1}{r}\frac{\partial(\rho U_\theta)}{\partial\theta}+\frac{\partial(\rho u_z)}{\partial z}=0 \qquad 3.4$$

The basic assumptions for deriving Reynolds equation are:

- The geometrical parameter of the fluid film in the bearing U_r and U_θ derivative with respect to z are much larger then derivative of other velocity component.
- External forces on the fluid film are zero.
- The inertia force and the body force terms are negligible compared with pressure force and viscous force terms.
- Flow of fluid in the bearing is viscous and laminar
- In the fluid-solid boundaries, there is no slip.
- Variation of pressure in the fluid film negligible which means

$$\frac{\partial p}{\partial z}=0$$

Combining Navier-Stoke equations (equations 3.1, 3.2 and 3.3) and continuity equation (equation 3.4) and consider the above basic assumptions, the generalized form of Reynolds equations can be found as equation 3.5.

$$\frac{\partial}{\partial r}\left(rh^3\frac{\partial p}{\partial r}\right)+\frac{1}{r}\frac{\partial}{\partial\theta}\left(h^3\frac{\partial p}{\partial\theta}\right)=6\eta U\frac{\partial h}{\partial\theta} \qquad 3.5$$

$$\text{Where } h = \begin{cases} C - C_{g,\text{Above the texture height}} \\ C, \text{else where} \end{cases}$$

C_g= Height of the texture and C = Total clearance

To find the non-dimensional form of Reynolds equation, h, r and p terms are non-dimesionalized as

$$\bar{h} = \frac{h}{c}, \bar{r} = \frac{r}{r_i} \text{ and } \bar{p} = \frac{pc^2}{\eta u r_i} \text{ in equation(5)}$$

$$\frac{\partial}{\partial \bar{r} r_i}\left(\bar{r} r_i (\bar{h}c)^3 \frac{\partial}{\partial r}\left(\frac{\bar{p}\eta u r_i}{c^2}\right)\right) + \frac{1}{\bar{r} r_i}\frac{\partial}{\partial \theta}\left((\bar{h}c)^3 \frac{\partial}{\partial \theta}\left(\frac{\bar{p}\eta u r_i}{c^2}\right)\right) = 6\eta u \frac{\partial \bar{h} c}{\partial \theta} \quad (3.6)$$

Rearrange equation (3.6)

$$\frac{\partial}{\partial \bar{r}}\left(\bar{r}\bar{h}^3 \frac{\partial \bar{p}}{\partial \bar{r}} \cdot \eta u c\right) + \frac{1}{r}\frac{\partial}{\partial \theta}\left(\bar{h}^3 \frac{\partial \bar{p}}{\partial \theta} \cdot \eta u c\right) = 6\eta u c \frac{\partial \bar{h}}{\partial \theta} \quad (3.7)$$

Expanding equation (3.7)

$$3\bar{r}\bar{h}^2 \frac{\partial \bar{h}}{\partial \bar{r}}\frac{\partial \bar{p}}{\partial \bar{r}} + \bar{r}\bar{h}^3 \frac{\partial^2 \bar{p}}{\partial \bar{r}^2} + \frac{3}{\bar{r}}\bar{h}^2 \frac{\partial \bar{h}}{\partial \theta}\frac{\partial \bar{p}}{\partial \theta} + \frac{\bar{h}^3}{r}\frac{\partial^2 \bar{p}}{\partial \theta} = 6\frac{\partial \bar{h}}{\partial \theta} \quad (3.8)$$

Now equation (3.8) describes variation of non-dimensional pressure profile in r and θ direction, which depends of variation of parameters like non-dimensional film thickness ratio, non-dimensional film thickness ratio in r and θ direction, Non dimensional radius. In Current research the textured surface chosen for analysis have above parameters to generate positive pressure profile.

3.2 Numerical Solution

There are many methods to solve non-dimensional Reynolds equation like Finite Element Method, Finite Volume Methods and Spectral Methods etc. Among all Finite Difference Method (FDM) is conceptually simple and uncomplicated to implement on a computer for regular shapes and fast iterative methods for solving this set of equations. So for current analysis FDM is used to solve Reynolds equation.

3.2.1 Finite Difference Method

The pressure distribution was calculated using the finite difference method. Then the system of numerical equations was solved iteratively using with help of the Gauss-Seidel method. The cavitations pressure was set to zero. This cavitations condition was integrated in the Gauss-Seidel iterative method so the Reynolds condition results by numerical diffusion. Central difference method is used in the present analysis, because it produces better estimates than forward or backward differences. All the differentials in the non-dimensionlized modified Reynolds equation are to be replaced by finite difference approximations using thin table 3.1.

$\frac{\partial \bar{h}}{\partial \theta}$	$\frac{\bar{h}(i,j+1)-\bar{h}(i,j-1)}{2\Delta\theta}$
$\frac{\partial \bar{h}}{\partial \bar{r}}$	$\frac{\bar{h}(i+1,j)-\bar{h}(i-1,j)}{2\Delta\bar{r}}$
$\frac{\partial \bar{p}}{\partial \bar{r}}$	$\frac{\bar{p}(i+1,j)-\bar{p}(i-1,j)}{2\Delta\bar{r}}$
$\frac{\partial \bar{p}}{\partial \theta}$	$\frac{\bar{p}(i,j+1)-\bar{p}(i,j-1)}{2\Delta\theta}$
$\frac{\partial^2 \bar{p}}{\partial \bar{r}^2}$	$\frac{\bar{p}(i-1,j)-2\bar{p}(i+1,j)+\bar{p}(i,j+1)}{\Delta\bar{r}^2}$
$\frac{\partial^2 \bar{p}}{\partial \theta^2}$	$\frac{\bar{p}(i,j-1)-2\bar{p}(i,j)+\bar{p}(i,j+1)}{\Delta\theta^2}$

Table 3.1: Finite Difference Toolkit for PDE.

Substituting values from table 3.1 in the equation (3.8)

$$3\bar{r}\bar{h}^2\left[\left(\frac{\bar{h}(i+1,j)-\bar{h}(i-1,j)}{2\Delta\bar{r}}\right)\left(\frac{\bar{p}(i+1,j)-\bar{p}(i-1,j)}{2\Delta\bar{r}}\right)\right]$$
$$+\bar{r}\bar{h}^3\left[\frac{\bar{p}(i-1,j)-2\bar{p}(i,j)+\bar{p}(i+1,j)}{\Delta\bar{r}^2}\right]$$
$$+\frac{3}{\bar{r}}\bar{h}^2\left[\left(\frac{\bar{h}(i,j+1)-\bar{h}(i,j-1)}{2\Delta\theta}\right)\left(\frac{\bar{p}(i,j+1)-\bar{p}(i,j-1)}{2\Delta\theta}\right)\right]$$
$$+\frac{\bar{h}^3}{\bar{r}}\left[\frac{\bar{p}(i,j-1)-2\bar{p}(i,j)+\bar{p}(i,j+1)}{\Delta\theta^2}\right]=6\left[\frac{\bar{h}(i,j+1)-\bar{h}(i,j-1)}{2\Delta\theta}\right] \quad (3.9)$$

$$2\bar{p}(i,j)\left[\frac{\bar{r}\bar{h}^3}{\Delta\bar{r}^2}+\frac{\bar{h}^3}{\bar{r}\Delta\theta^2}\right]+\frac{3}{\Delta\theta}\left[\bar{h}(i,j+1)-\bar{h}(i,j-1)\right]$$

$$=\frac{3\bar{r}\bar{h}^2}{(2\Delta\bar{r})^2}\left[\bar{h}(i+1,j)-\bar{h}(i-1,j)\right]*\left[\bar{p}(i+1,j)-\bar{p}(i-1,j)\right]$$

$$+\frac{\bar{r}\bar{h}^3}{\Delta\bar{r}^2}\left[\bar{p}(i-1,j)+\bar{p}(i+1,j)\right]$$

$$+\frac{3\bar{h}^2}{2\bar{r}\Delta\theta}\left[\left\{\bar{h}(i,j+1)-\bar{h}(i,j-1)\right\}\left\{\bar{p}(i,j+1)-\bar{p}(i,j-1)\right\}\right]$$

$$+\frac{\bar{h}^3}{\bar{r}\Delta\theta^2}\left[\bar{p}(i,j-1)+\bar{p}(i,j-1)\right]-\frac{3}{\Delta\theta}\left[\bar{h}(i,j+1)-\bar{h}(i,j-1)\right] \qquad (3.10)$$

$$\bar{p}(i,j)\left[\frac{2\bar{h}}{\Delta\bar{r}^2}+\frac{2\bar{h}}{\bar{r}^2\Delta\theta^2}\right]$$

$$=\frac{3}{(2\Delta\bar{r})^2}\left[\bar{h}(i+1,j)-\bar{h}(i-1,j)\right]\left[\bar{h}(i+1,j)-\bar{p}(i-1,j)\right]$$

$$+\frac{\bar{h}}{\Delta\bar{r}^2}\left[\bar{p}(i-1,j)+\bar{p}(i+1,j)\right]$$

$$+\frac{3}{\bar{r}^2(2\Delta\theta)^2}\left[\bar{h}(i,j+1)-\bar{h}(i,j-1)\right]\left[\bar{p}(i,j+1)-\bar{p}(i,j-1)\right]$$

$$+\frac{\bar{h}}{\bar{r}^2\Delta\theta^2}\left[\bar{p}(i,j-1)+\bar{p}(i,j+1)\right]-\frac{3}{\bar{h}^2\bar{r}\Delta\theta}\left[\bar{h}(i,j+1)-\bar{h}(i,j-1)\right] \qquad (3.11)$$

$$\bar{p}(i,j)=\frac{\mathrm{A}+\mathrm{B}+\mathrm{C}+\mathrm{D}-\mathrm{E}}{\mathrm{G}} \qquad (3.12)$$

Where

$$\mathrm{A}=\frac{3}{(2\Delta\bar{\mathrm{r}})^2}\left[\bar{\mathrm{h}}(\mathrm{i}+1,\mathrm{j})-\bar{\mathrm{h}}(\mathrm{i}-1,\mathrm{j})\right]\left[\bar{\mathrm{h}}(\mathrm{i}+1,\mathrm{j})-\bar{\mathrm{p}}(\mathrm{i}-1,\mathrm{j})\right]$$

$$\mathrm{B}=\frac{\bar{\mathrm{h}}}{\Delta\bar{\mathrm{r}}^2}\left[\bar{\mathrm{p}}(\mathrm{i}-1,\mathrm{j})+\bar{\mathrm{p}}(\mathrm{i}+1,\mathrm{j})\right]$$

$$\mathrm{C}=\frac{3}{\bar{\mathrm{r}}^2(2\Delta\boldsymbol{\theta})^2}\left[\bar{\mathrm{h}}(\mathrm{i},\mathrm{j}+1)-\bar{\mathrm{h}}(\mathrm{i},\mathrm{j}-1)\right]\left[\bar{\mathrm{p}}(\mathrm{i},\mathrm{j}+1)-\bar{\mathrm{p}}(\mathrm{i},\mathrm{j}-1)\right]$$

$$\mathrm{D}=\frac{\bar{\mathrm{h}}}{\bar{\mathrm{r}}^2\Delta\theta^2}\left[\bar{\mathrm{p}}(\mathrm{i},\mathrm{j}-1)+\bar{\mathrm{p}}(\mathrm{i},\mathrm{j}+1)\right])$$

$$\mathrm{E} = \frac{3}{\bar{h}^2 \bar{r} \Delta\theta}\left[\bar{h}(i, j+1) - \bar{h}(i, j-1)\right]$$

$$\mathrm{G} = \frac{2\bar{\mathrm{h}}}{\Delta\bar{\mathrm{r}}^2} + \frac{2\bar{\mathrm{h}}}{\bar{\mathrm{r}}^2 \Delta\theta^2}$$

First the pressure distribution is calculated then the non-dimensional load carrying capacity, non-dimensional frictional force and coefficient friction parameter is calculated using the expression below:

Non-dimensional friction force, $\bar{F}$

$$\bar{\mathrm{F}} = \frac{FC}{\eta U {r_i}^2} = \iint \left(\frac{\bar{h}}{2}\frac{\partial \bar{p}}{\partial \theta} + \frac{\bar{r}}{\bar{h}}\right) d\theta d\bar{r} \qquad (3.13)$$

Non-dimensional load, $\bar{W}$

$$\bar{W} = \frac{WC^2}{\eta U {r_i}^3} = \iint \bar{p}\bar{r} d\bar{r} d\theta \qquad (3.14)$$

Coefficient friction parameter, f

$$f = \frac{\bar{F}}{\bar{W}} \qquad (3.15)$$

3.3 Flow Chat

The Flow Chat is shown in figure 3.1, which will help to write code in MATLAB, to find non-dimensional load and coefficient of friction parameter for different aspect ratio and height ratio.

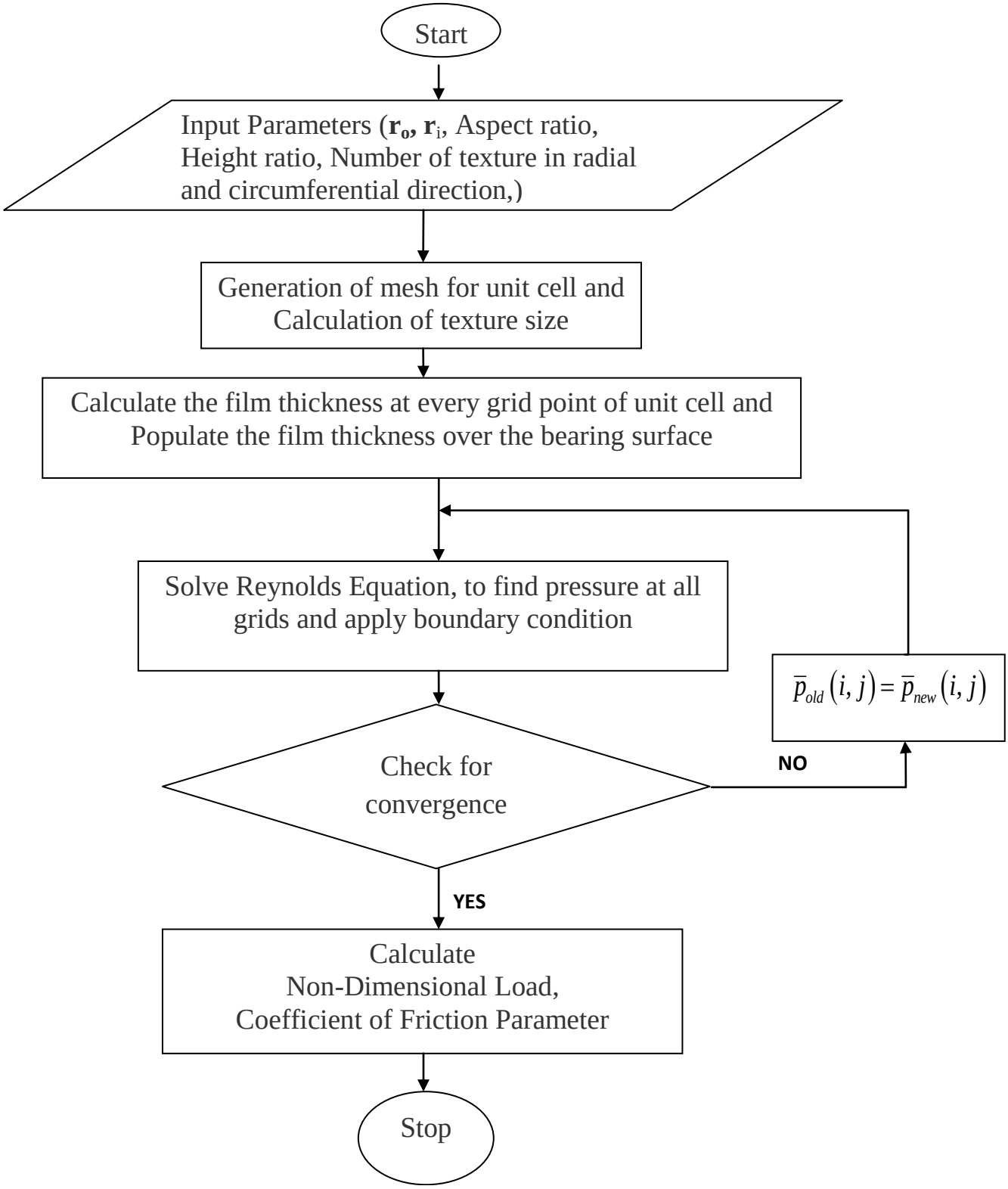

CHAPTER 4

4. Results and Discussion

Theoretical and graphical analysis is carried out to study the performance characteristics of the hydrodynamic thrust pad bearing .In the present analysis effect of aspect ratio, texture height ratio on non dimensional load and coefficient of friction parameter is done.

What is Aspect Ratio and Texture Height Ratio?

For numerical analysis, the bearing surface is modeled by dividing into finite number of squares (unit cell) which are equal to number of asperities, i.e. each unit cell contain one asperity. Aspect Ratio is defined as ratio of projected area of asperities to total area of square. Similarly each asperity has some height, when the maximum height of the asperity is divided by the width of the unit cell it gives the texture height ratio. Figure 4.1 shows asperities with different aspect ratio and height ratio for better understanding of the terms.

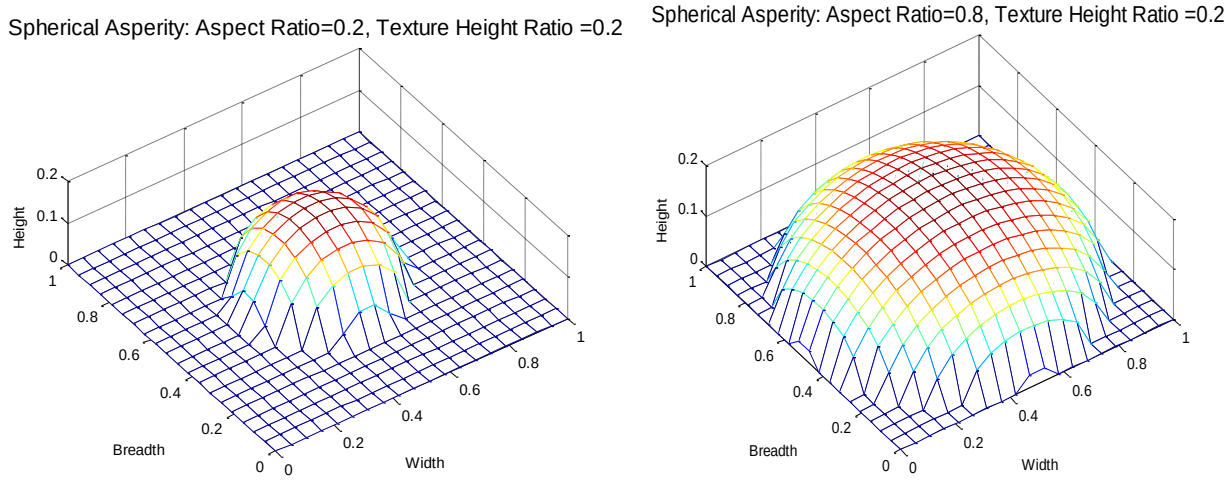

Fig 4.1: Modelling with different Aspect Ratio and Texture Height Ratio

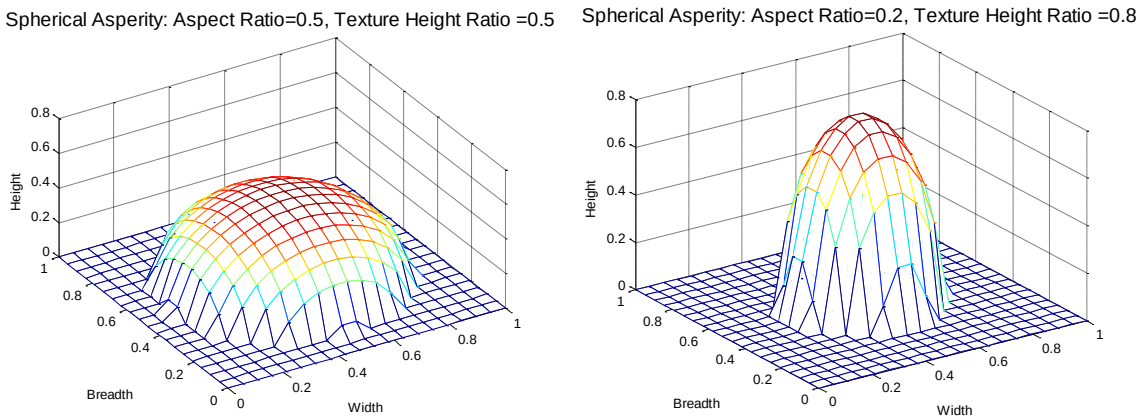

Fig 4.2: Modelling with different Aspect Ratio and Texture Height Ratio

surface is shown in the figure 4.2 and 4.3 respectively. Validation of numerical solution is carried out by making texture height ratio zero and aspect ratio zero that means a case of plain thrust pad bearing with that of previously available results. Next section follows with result for different texture profile to find the effect of texture profile in non-dimensional load carrying capacity and coefficient of friction parameter.

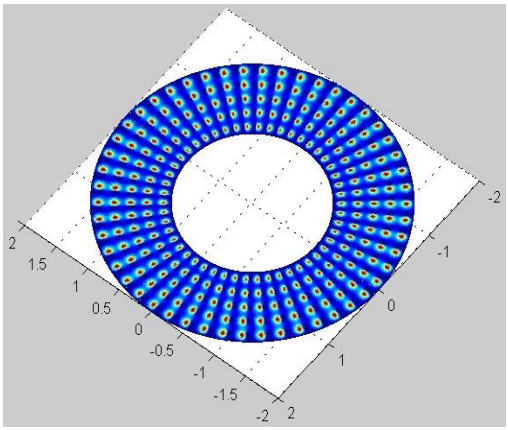

Figure- 4.2: Distribution of texture radially and circumferentially.

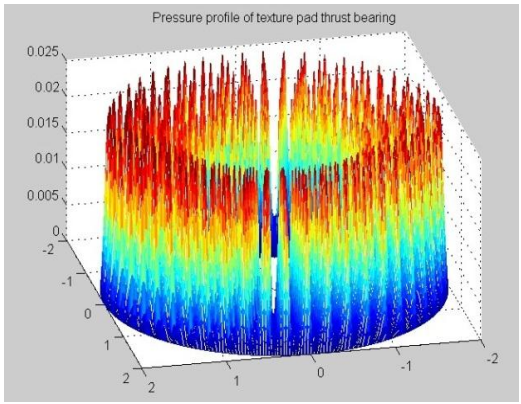

Figure- 4.3: Pressure Distribution over texture profile.

4.1. Spherical Texture

Spherical Asperities can be of positive type or negative type; both cases are modeled and analyzed for the performance parameter.

4.1.1. Positive Asperities

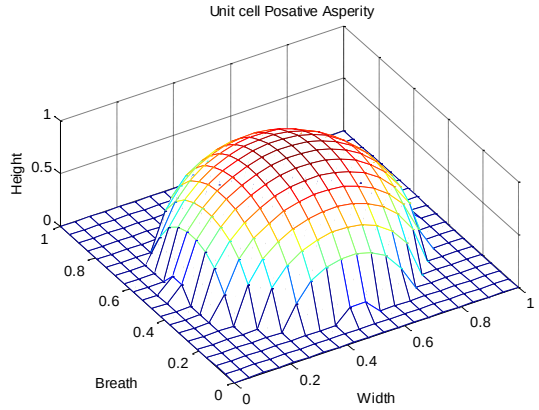

Fig: 4.1.1: Single Positive Spherical asperity

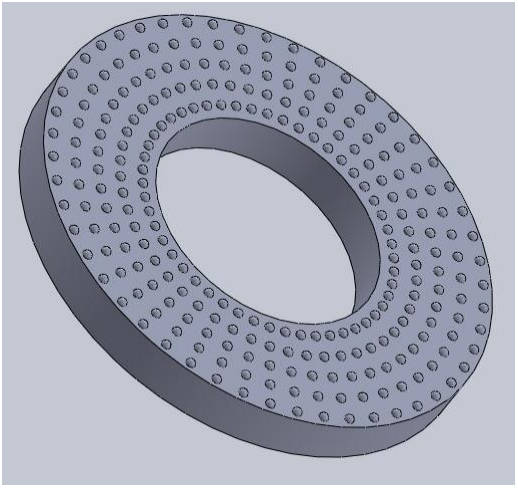

Fig: 4.1.2: Distribution of Positive Spherical Asperities.

These are micron scaled surface featured with spherical protrusion on a surface. Model of a single positive spherical asperity is shown in figure 4.1.1.The distribution of engineered spherical textures over complete thrust bearing surface is shown in figure 4.1.2.

(a)Effect of Aspect Ratio on Non-Dimensional Load and Coefficient of friction Parameter

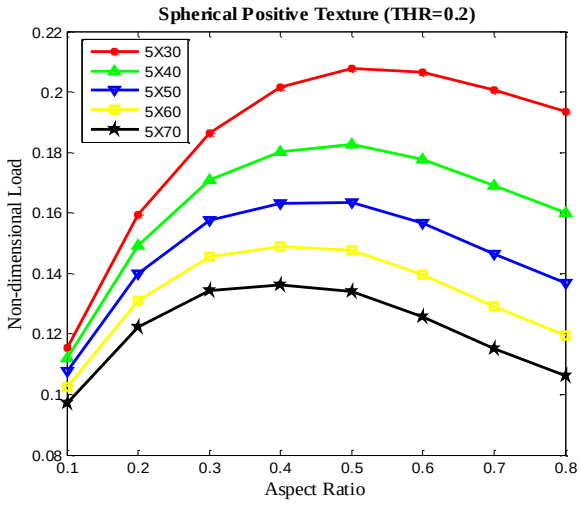

Fig 4.1.3:Non-dimensional load Vs. Aspect ratio for different distribution of positive spherical texture.

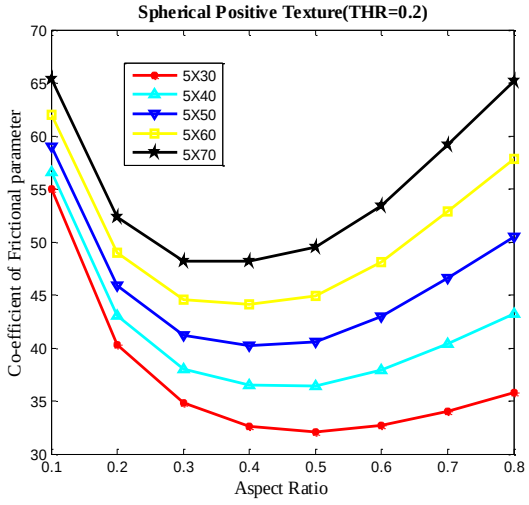

Fig 4.1.4: Coefficient of friction parameter Vs. aspect ratio for different distribution of positive spherical texture.

Effect of Aspect Ratio on Non-dimensional Load

Hydrodynamic analysis for non-dimensional load on spherical textured thrust bearing is plotted in figure 4.1.3, which shows increase in non dimensional load carrying capacity with increase in aspect ratio, This is due to increase of roughness or increases in asperity interaction with adjacent asperity which result increase in pressure over the bearing surface so load carrying capacity increase. The load carrying capacity increase up to a certain value of aspect ratio (0.4 to 0.6), after that load carrying value decrease for higher value of the aspect ratio .The drop in load carrying capacity with increase in aspect ratio beyond a limiting value is because of smoothness of bearing surface. Figure 4.1.3 also indicates increase in load carrying capacity with decrease in texture density. When the less number of texture present in the bearing surface it behave like rough surface so the load carrying capacity is high .How ever if the number of texture is very high or very small ,the bearing surface behaves as smooth surface so the load carrying capacity decrease in bearing. This shows there is limiting value of aspect ratio as well as texture density for maximum load carrying capacity for a specific texture height ratio.

Effect of Aspect Ratio on Coefficient Friction Parameter

Figure 4.1.4 shows variation of coefficient friction parameter with the aspect ratio. Coefficient of friction parameter decrease with increase of aspect ratio, however it has a limiting value, on further increase the aspect ratio again the coefficient of friction increase. The limiting value is in the range of 0.4 to 0.6. For very low value of aspect ratio the roughness of pad surface is low, so load carrying capacity is small but frictional force is high so coefficient of friction is high. But when aspect ratio increases load carrying capacity increases hence coefficient of friction decreases. However further increase the aspect ratio the bearing surface act as very smooth surface so macroscopically roughness decreases so that adhesion force between lubricant and solid surface increases as a result coefficient friction increase. Coefficient of friction also depends on texture density, when texture density increases coefficient of friction increase.

(b). Effect of Texture Height Ratio on Non-Dimensional Load and Coefficient of Friction parameter

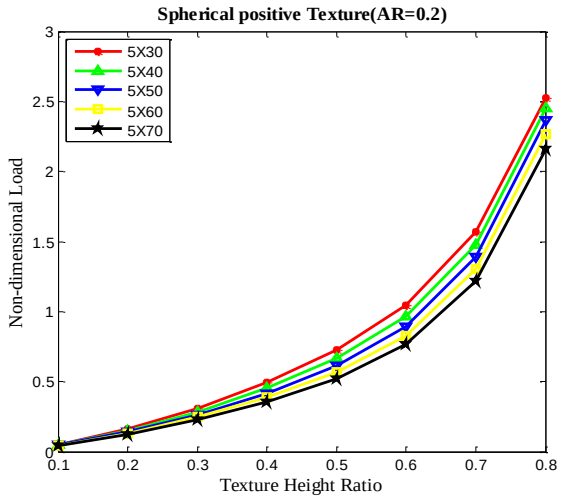

Fig 4.1.5:Non-Dimensional load Vs. Texture height ratio for different distribution of positive spherical texture.

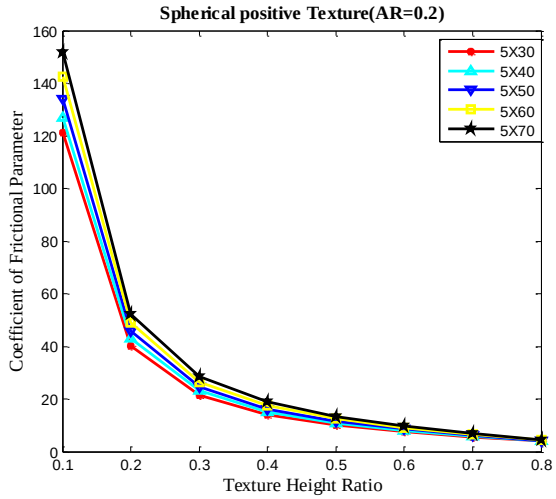

Fig 4.1.6: Coefficient of friction parameter Vs.Texture height for different distribution of positive spherical texture.

Effect of Texture Height Ratio on Non-dimensional Load

Figure 4.1.5 shows non dimensional load of the bearing increase with increase in the texture height. .The increase in the texture height of the bearing restricts the flow of lubrication so cross-sectional area of flow of lubrication decrease due to decrease in cross-sectional area pressure in the bearing increase. The increase in pressure results in increase of non-dimensional load. Increase in texture density the bearing acts as smooth surface so the load carrying capacity of the bearing decrease.

Effect of Texture Height Ratio on Coefficient of Friction parameter

Coefficient of friction parameter in the bearing surface decrease with increase the texture height of the bearing(Figure 4.1.6).When the texture height increase the roughness of the bearing surface increase so adhesion force between lubricant and bearing surface decrease so coefficient of friction decrease. With increase in texture density co efficient of friction increase this is due to

increase in texture density roughness of the bearing surface decrease. The texture height ratio has to be maintained above 20% for smaller coefficient of friction.

4.1.2. Negative Asperities

In the analysis negative spherical asperity is also included to compare with positive type asperities, Figure 4.1.7 show modeling of unit cell.

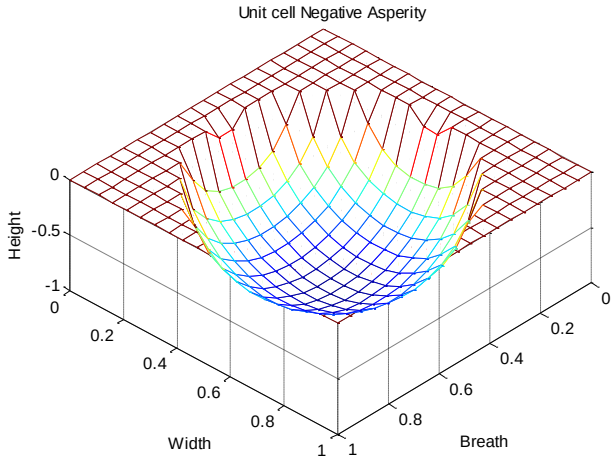

Fig: 4.1.7: Single Negative Spherical Asperity

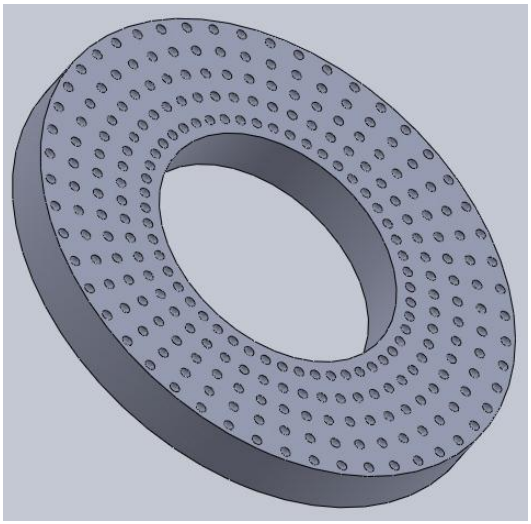

Fig: 4.1.8: Distribution of Negative Spherical Asperities.

Effect of Aspect Ratio on Non-Dimensional Load and Coefficient of Friction parameter

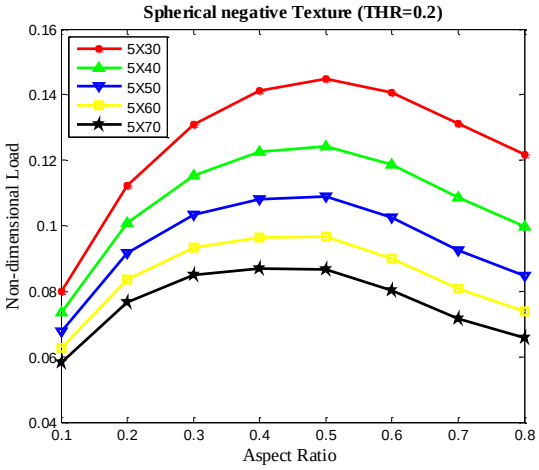

Fig 4.1.9: Non-Dimensional load Vs.Aspect ratio for different distribution of negative spherical texture.

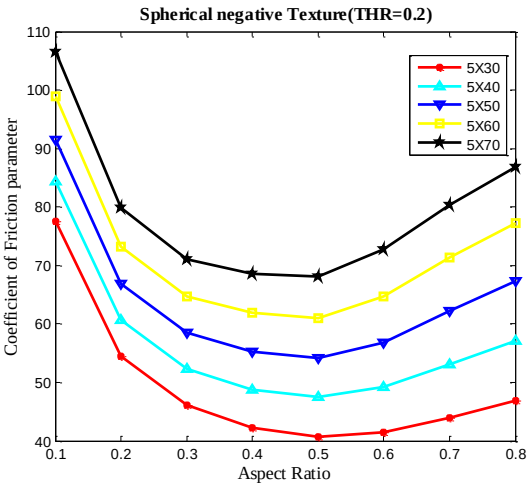

Fig 4.1.10: Coefficient of friction parameter Vs. Aspect ratio for different distribution of negative spherical texture.

Effect of Texture Height Ratio on Non-Dimensional Load and Coefficient of Friction parameter

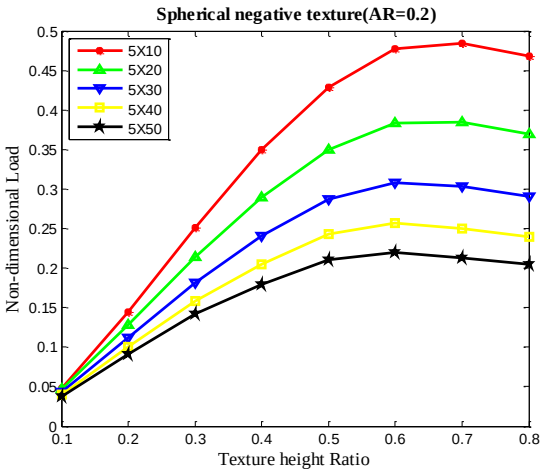

Fig 4.1.11 Non-Dimensional load Vs. Texture height ratio for different distribution of negative spherical texture.

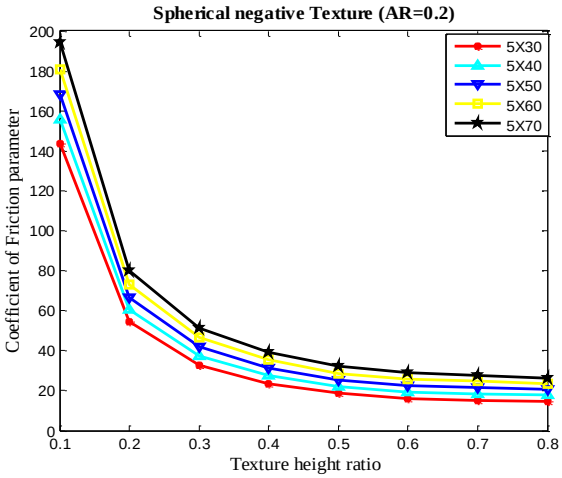

Fig 4.1.12: Coefficient of friction parameter Vs. Texture height ratio for different distribution of negative spherical texture.

Effect of Aspect Ratio on Non-dimensional Load

The non-dimensional load for negative asperity shows same type of behavior as positive type asperity(figure 4.1.9), However for the same texture density the Non dimensional load is lower than the positive type of asperity.

Effect of Aspect Ratio on Coefficient Friction parameter

Figure 4.1.10 shows effect of aspect ratio on coefficient of friction decrease. The behavior of curves is same as positive type asperity, but for the same texture density the coefficient friction parameter is very high in negative type asperity.

Effect of Texture Height Ratio on Non dimensional load

Figure 4.1.11 shows higher rate of increase in non-dimensional load in negative type spherical asperity compare with positive type, this is due better texture interaction between adjacent textures.

Effect of Texture Height Ratio on Coefficient of Friction parameter

The coefficient of friction decreases with increase in texture height ratio (figure 4.1.12), at very high texture height ratio the minimum film thickness is close to texture height, so rate of change of coefficient friction is small.

The above analysis shows, the non-dimensional load of positive spherical texture is better that negative type for chosen texture density. The coefficient of friction is found to very high for aspect ratio and texture height ratio less than 20%. The non-dimensional load and coefficient of friction parameter largely depends on aspect ratio, texture height ratio and texture density.

4.2. Cylindrical Texture

4.2.1. Positive asperities

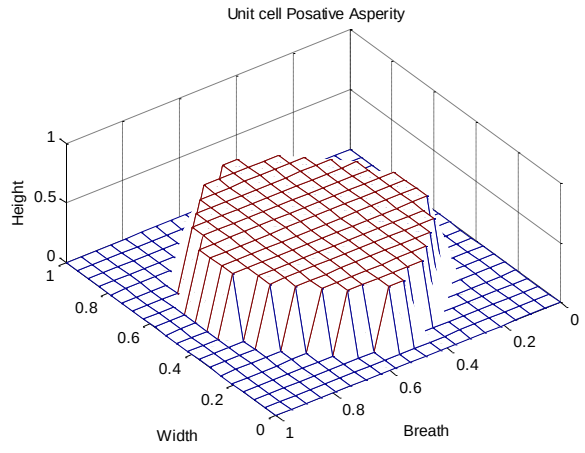

Fig 4.2.1: Single Positive Cylindrical Asperity

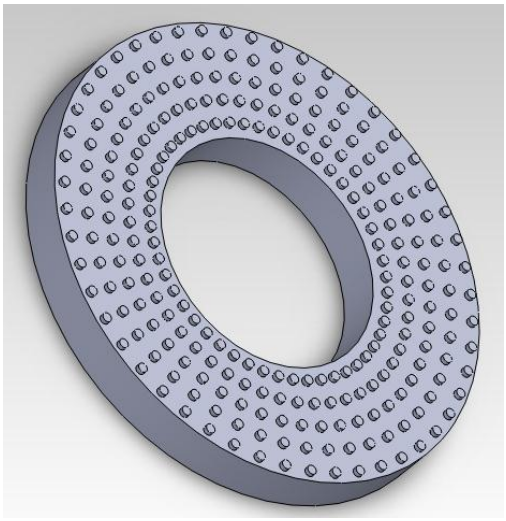

Fig 4.2.2: Distribution of Positive Cylindrical Asperities

Effect of Aspect Ratio on Non Dimensional Load and Coefficient of Frictional parameter

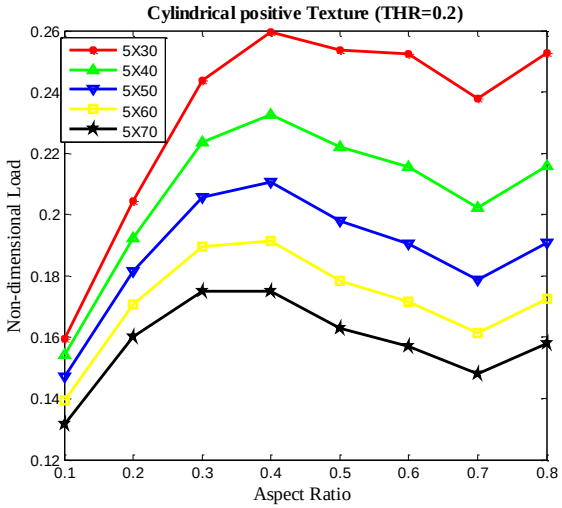

Fig 4.2.3: Non-Dimensional Load Vs. Aspect ratio for different distribution of positive cylindrical texture.

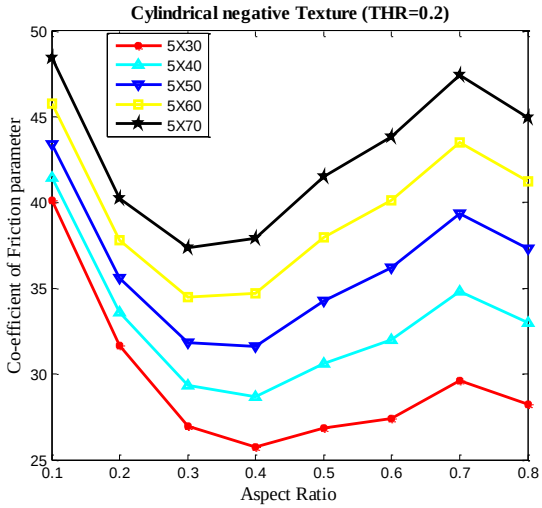

Fig 4.2.4:Coefficient of friction parameter Vs. Aspect ratio for different distribution of positive cylindrical texture.

Effect of Texture Height Ratio on Non Dimensional Load and Coefficient of Friction parameter

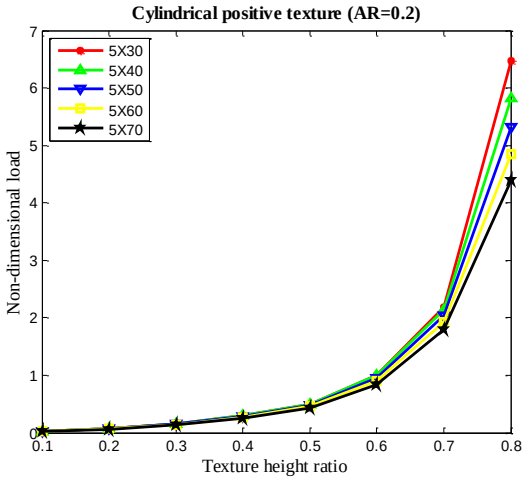

Fig 4.2.5:Non-Dimensional load Vs. Texture height ratio for different distribution of positive cylindrical texture.

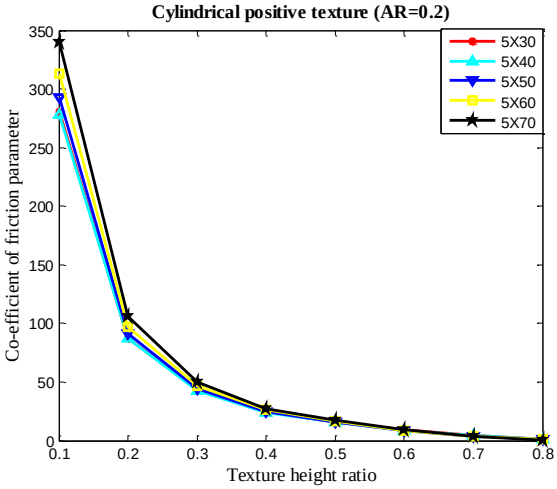

Fig 4.2.6: Coefficient of friction parameter Vs. Texture height ratio for different distribution of positive cylindrical texture.

Effect of aspect ratio and texture height ratio for cylindrical positive texture is shown from figure 4.2.3 to 4.2.6 .The non-dimensional load is found to much better in cylindrical positive texture

profile compared with spherical positive texture. The texture height in cylindrical texture has very high impact on non-dimensional load.

4.2.2. Negative Asperities

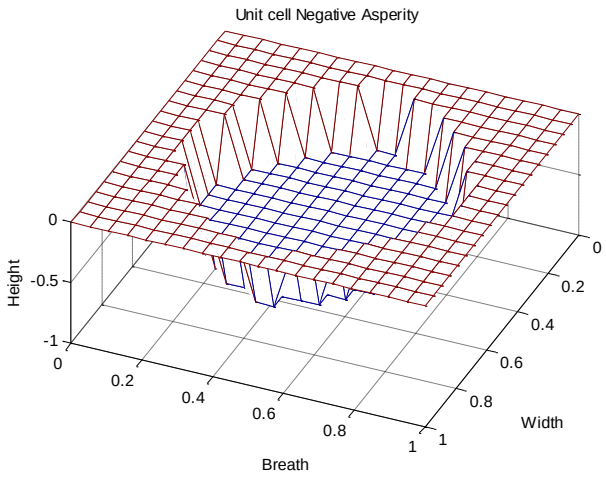

Fig 4.2.7: Single Negative Cylindrical Asperity

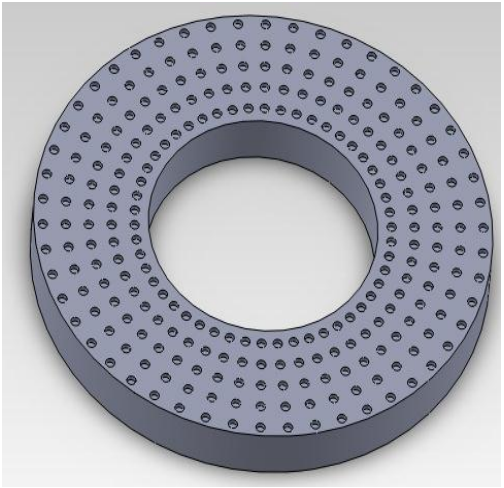

Fig 4.2.8: Distribution of Negative Cylindrical Asperities

Effect of Aspect Ratio on Non Dimensional Load and Coefficient of friction parameter

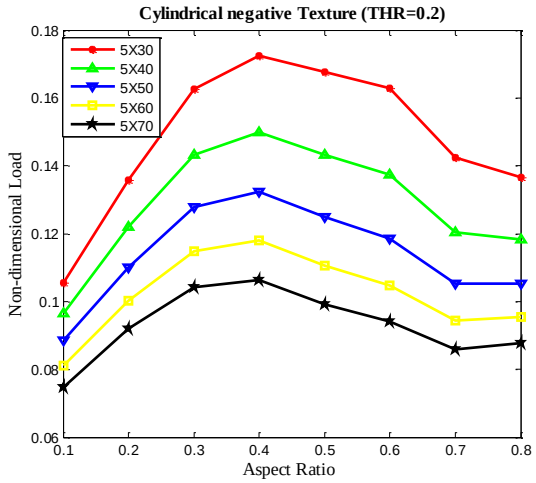

Fig 4.2.9:Non-dimensional load Vs aspect ratio for different distribution of negative cylindrical texture.

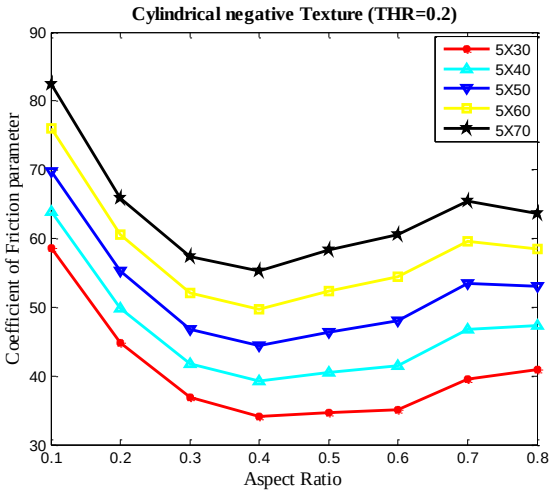

Fig 4.2.10:Coefficient of friction parameter Vs. Aspect ratio for different distribution of negative cylindrical texture.

Effect of Texture Height Ratio on Non dimensional Load and Coefficient of Friction parameter

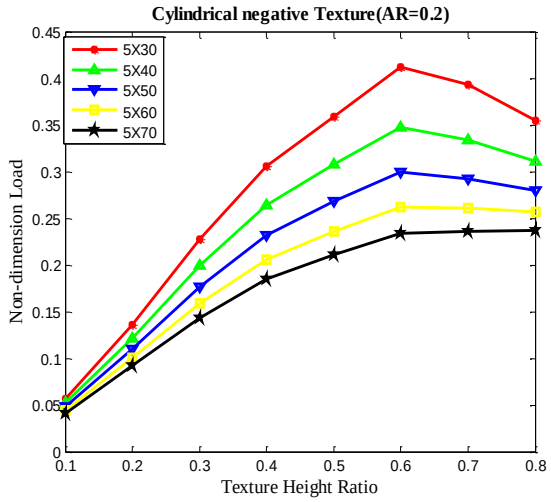

Fig 4.2.11: Non-Dimensional load Vs. Texture height ratio for different distribution of negative cylindrical texture.

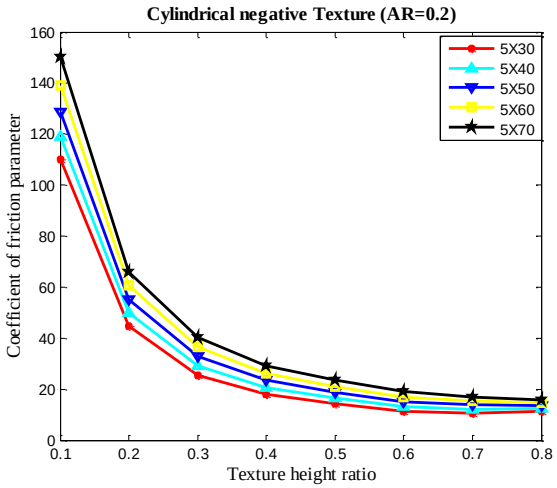

Fig 4.2.12: Coefficient of friction parameter Vs. Texture height ratio for different distribution of negative cylindrical texture.

From figure 4.2.9 to 4.2.12 it shown the effect of aspect ratio and texture height ratio on load carrying capacity and co-efficient of friction parameter of cylindrical negative texture .The load carrying capacity is found to be less in cylindrical negative texture profile compared to spherical positive texture. It also shows coefficient of friction parameter is high compared to the positive cylindrical texture.

4.3. Elliptical Texture

4.3.1. Positive asperities

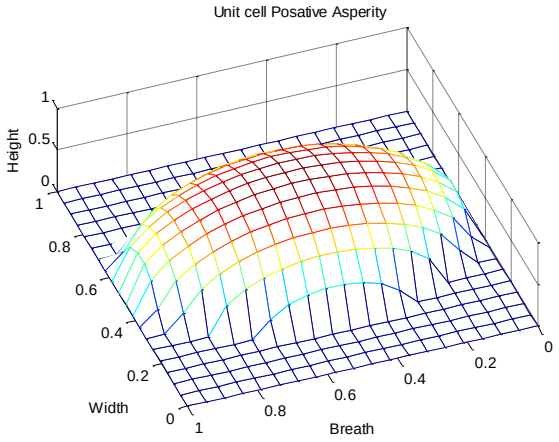

Fig 4.3.1: Single Positive Elliptical Asperity

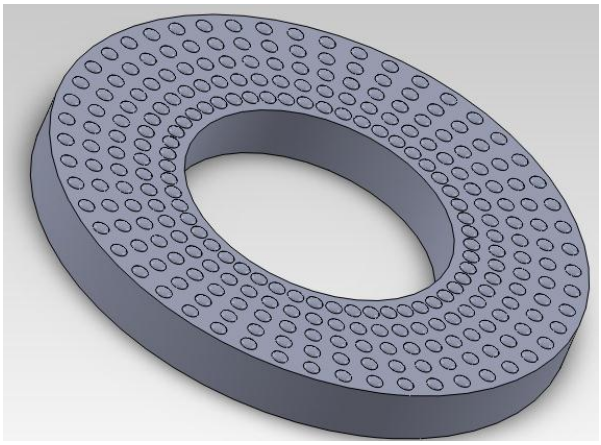

Fig 4.3.2: Distribution of Positive Elliptical Asperities

Effect of Aspect Ratio on Non Dimensional Load and Coefficient of Friction parameter

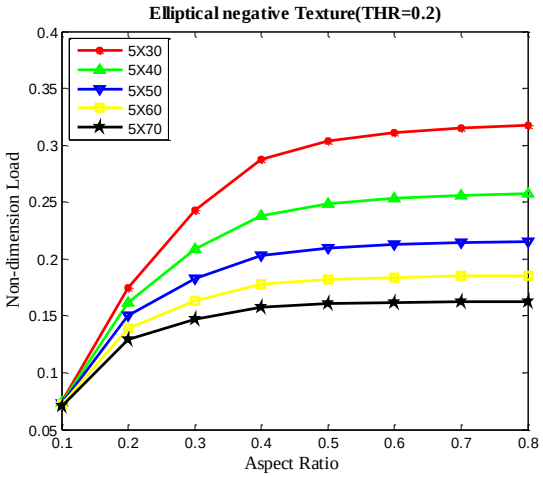

Fig 4.3.3:Non-dimensional load Vs. Aspect ratio for different distribution of positive elliptical texture.

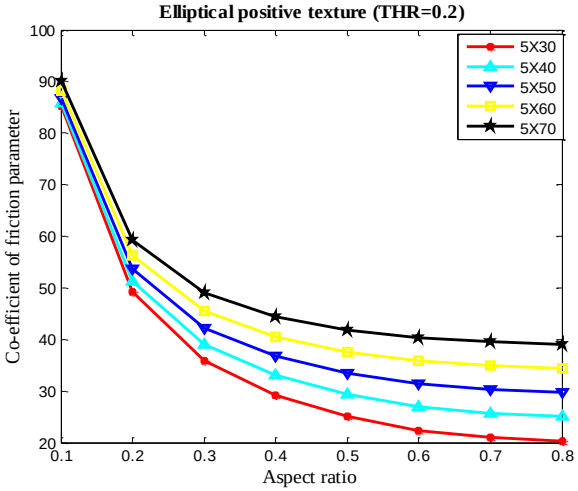

Fig 4.3.4: Coefficient of Friction parameter Vs. Aspect ratio for different distribution of positive elliptical texture.

Effect of Texture Height Ratio on Non Dimensional Load and Coefficient Friction parameter

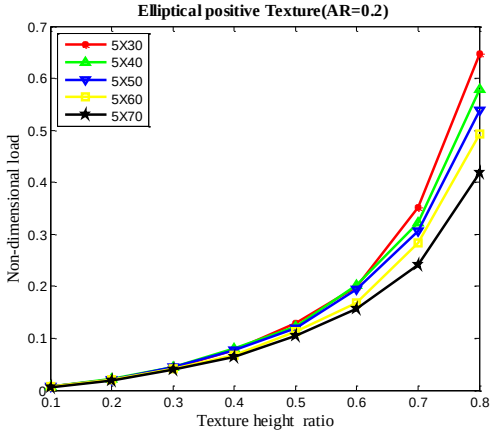

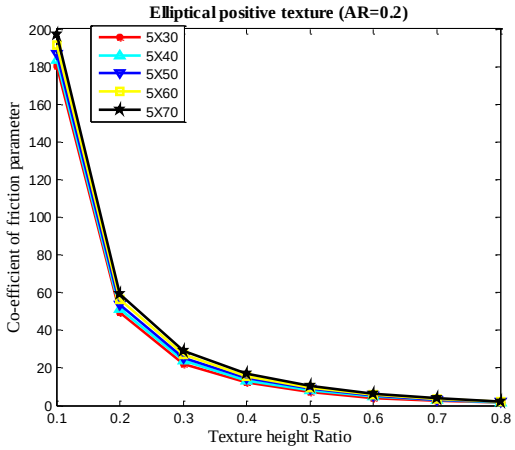

Fig 4.3.5: vs. Non-Dimensional Load Vs. Texture height ratio for different distribution of Positive Elliptical texture.

Fig 4.3.6: Coefficient of Frictional parameter Vs. Texture height ratio for different distribution of positive Elliptical texture.

Non-dimension load and Coefficient of friction parameter versus aspect ratio and texture height ratio for elliptical positive asperity are plotted in the figure from 4.3.3 to 4.3.6 .The non-dimensional load is higher compared to cylindrical texture and coefficient of friction parameter of elliptical positive texture profile have low compared with cylindrical positive texture when they are compared with aspect ratio but when they are compare with texture height ratio non dimensional load value low. The texture height in elliptical texture has very high impact on non-dimensional load and coefficient of friction parameter then aspect ratio.

4.3.2. Negative Asperity

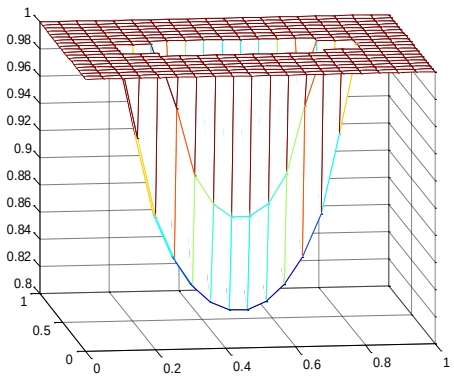

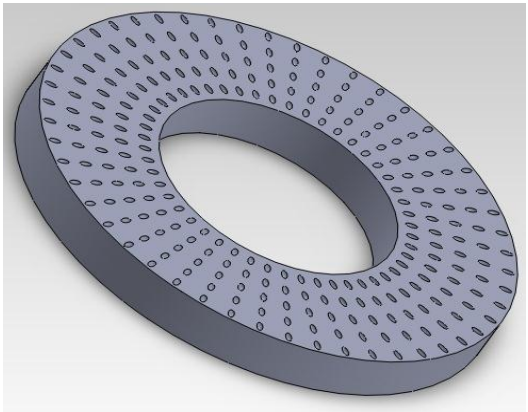

Fig 4.3.7: Single Negative Elliptical Asperity

Fig 4.3.8: Distribution of Negative Elliptical Asperities

Effect of Aspect Ratio on Non dimensional load and Coefficient of Friction parameter

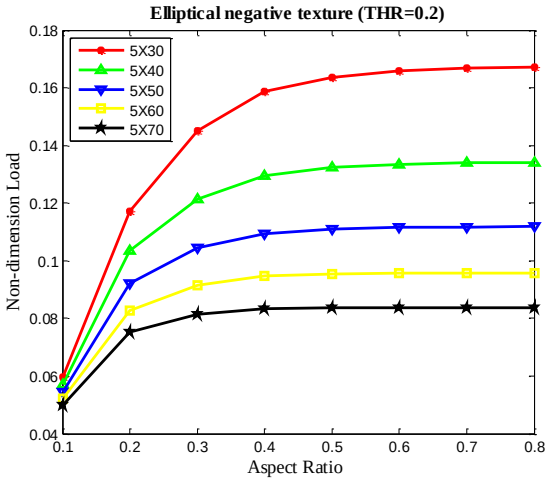

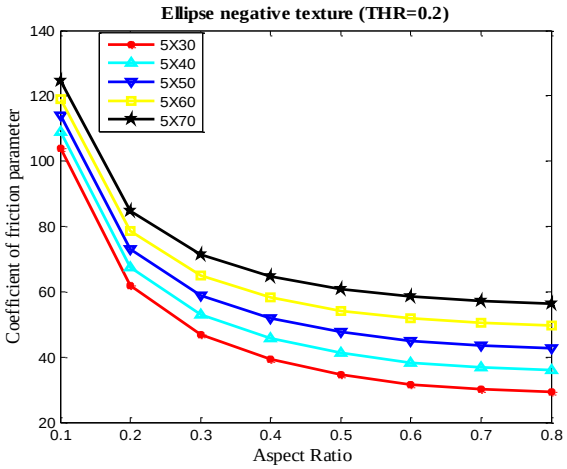

Fig 4.3.9:Non-Dimensional load Vs. Aspect ratio for different distribution of Negative elliptical texture.

Fig 4.3.10: Coefficient of friction parameters Vs. Aspect ratio for different distribution of Negative elliptical texture.

Effect of Texture Height Ratio on Non dimensional Load and Coefficient Friction parameter

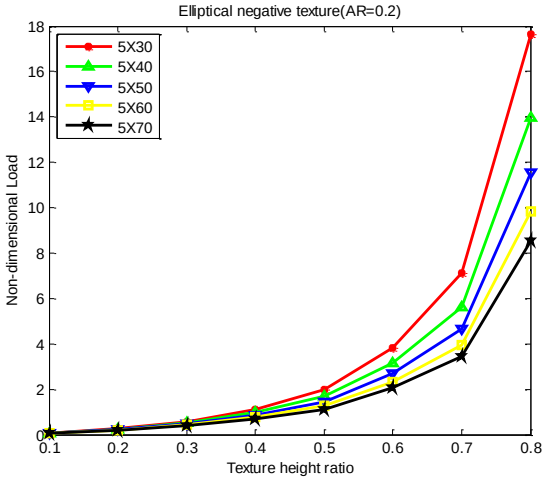

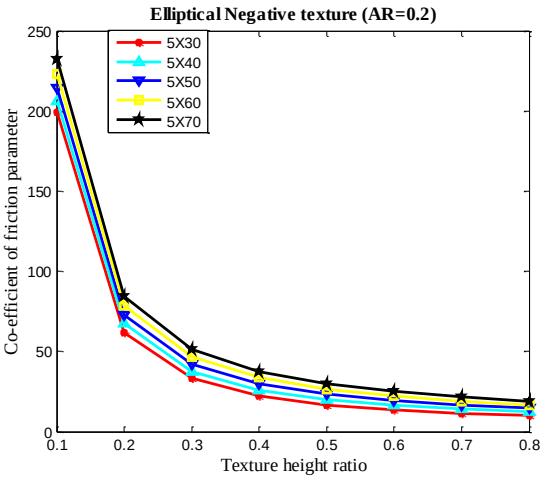

Fig 4.3.11: Non-Dimensional Load Vs. Texture height ratio for different distribution of negative elliptical texture.

Fig 4.3.12: Coefficient of Friction parameter Vs. Texture height for different distribution of negative elliptical texture.

Effect of aspect ratio and texture height ratio for elliptical negative texture is shown from figure 4.3.9 to 4.3.12 .The non-dimensional load is low and coefficient of friction parameter is high in

elliptical negative texture profile compared with elliptical positive texture. Like other structure elliptical negative texture has high impact on load carrying capacity with Texture Height Ratio.

4.4. Rectangular Texture

4.4.1. Positive asperity

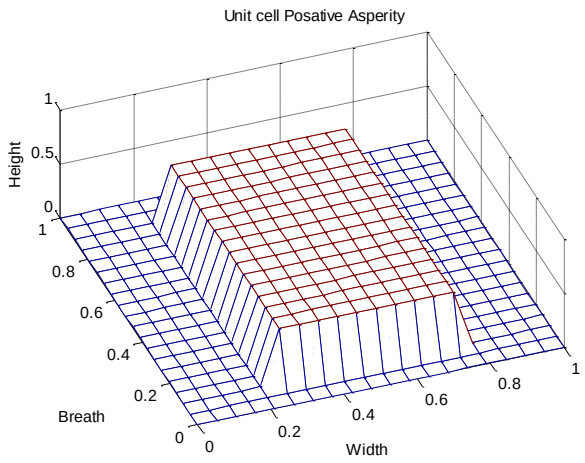

Figure 4.4.1: Single Positive Rectangle Asperity

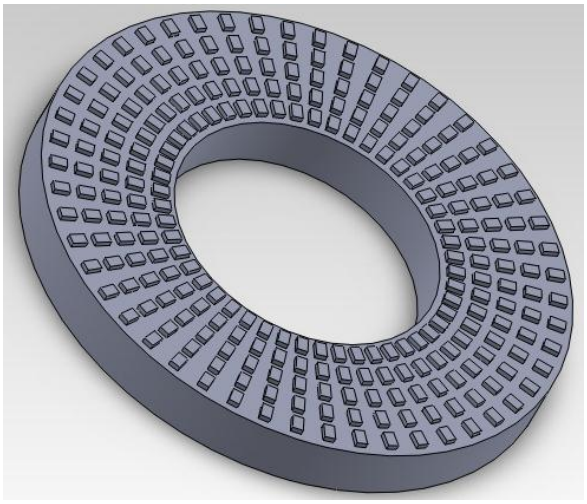

Figure 4.4.2: Distribution of Positive Rectangle Asperities

Effect of Aspect Ratio on Non dimensional Load and Coefficient of Friction parameter

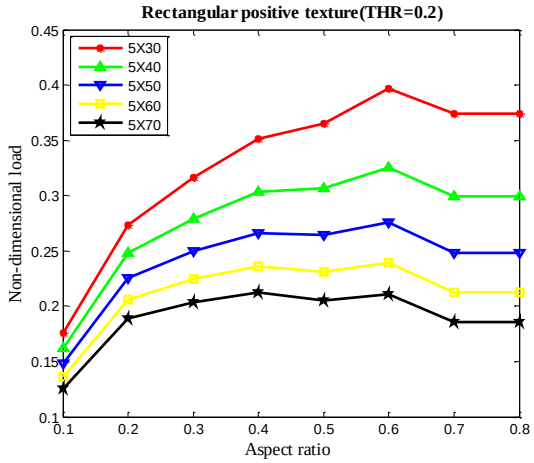

Fig 4.4.3:Non-Dimensional load Vs. Aspect ratio for different distribution of positive rectangle texture.

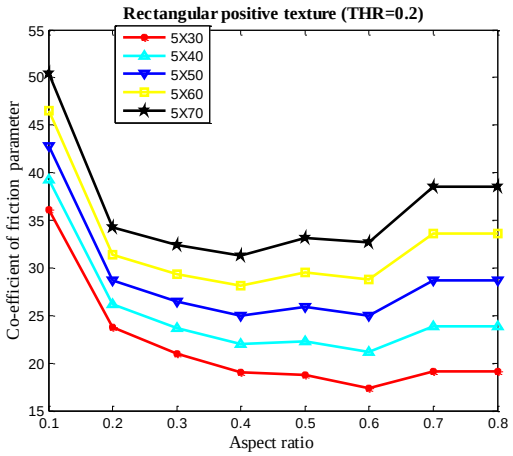

Fig 4.4.4: Coefficient of friction parameter Vs. Aspect ratio for different distribution of positive rectangle texture.

Effect of Texture Height Ratio on Non-dimensional Load and Coefficient of Frictional parameter

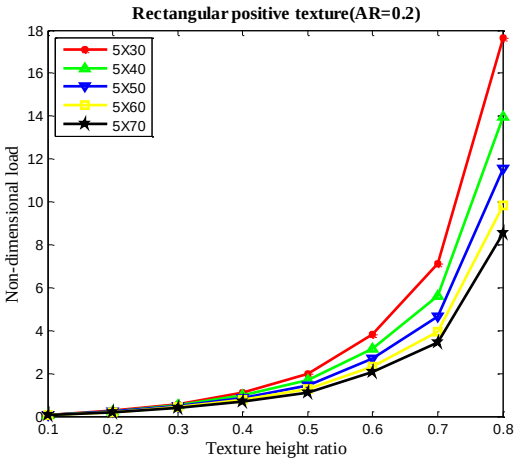

Fig 4.4.5: Non-Dimensional load Vs. Texture height ratio for different distribution of positive rectangle texture.

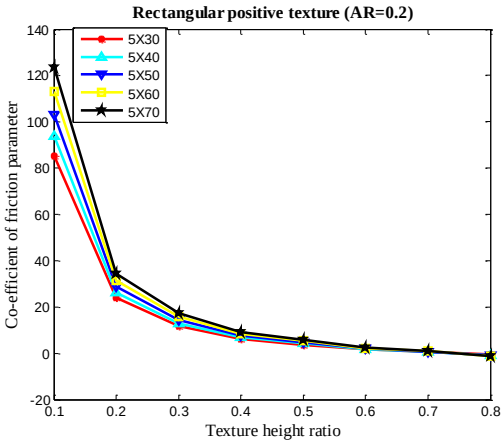

Fig 4.4.6: vs. Coefficient of friction parameter Vs. Texture height ratio for different distribution of positive rectangle texture.

Non-dimensional load and coefficient of friction parameter versus aspect ratio and texture height ratio for rectangle positive asperity are plotted in the figure from 4.3.3 to 4.3.6 .The non-dimensional load is very high and coefficient of Friction parameter is very low in rectangular positive texture profile compared with other Texture .

4.4.2. Negative Asperity

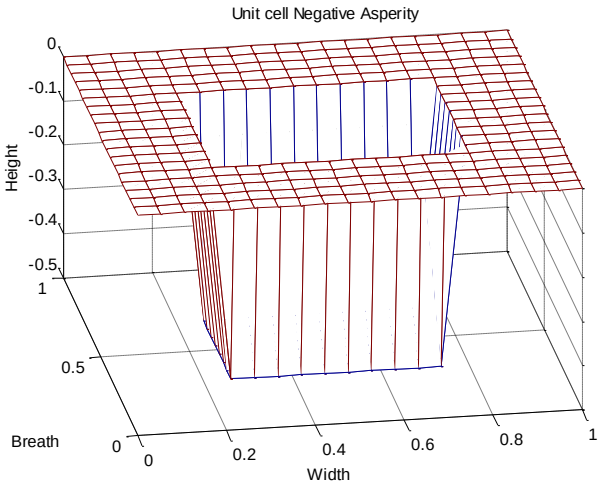

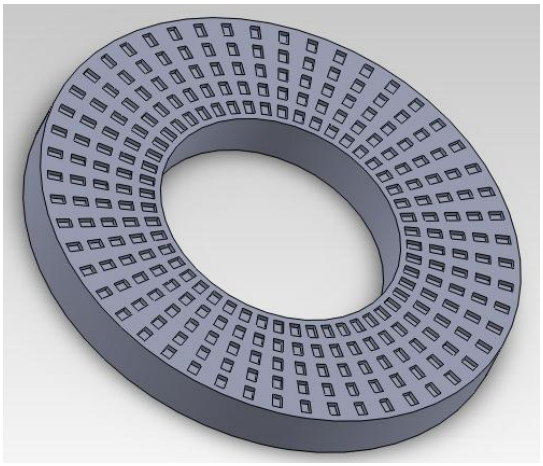

Fig 4.4.7: Single Negative Rectangle Asperity

Fig 4.4.8: Distribution of Negative Rectangle Asperities

Effect of Aspect Ratio on Non-dimensional load and Coefficient of Friction parameter

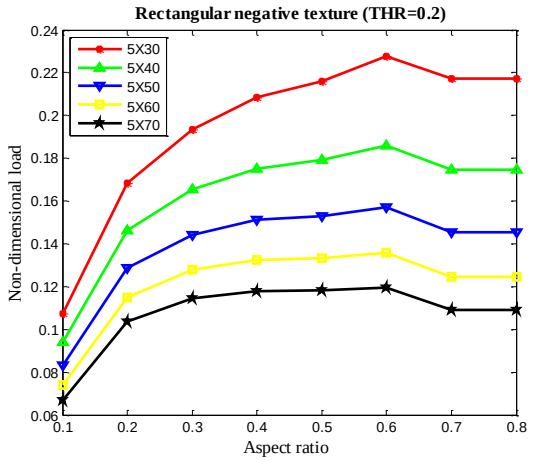

Fig 4.4.9:Non-dimensional load Vs. Aspect ratio for different distribution of negative rectangle texture.

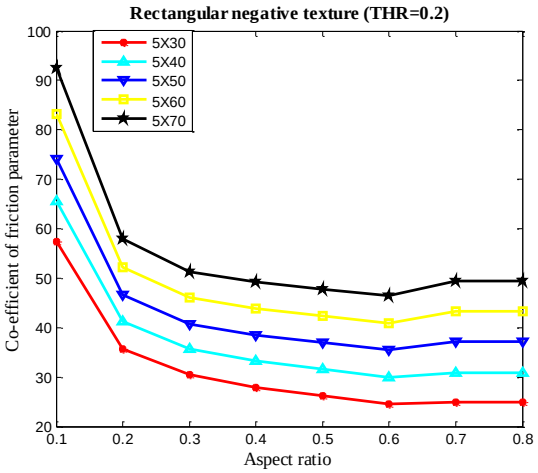

Fig 4.4.10: Coefficient of friction parameter Vs. Aspect ratio for different distribution of negative rectangle e texture.

Effect of Texture Height Ratio on Non-dimensional Load and Coefficient of Friction parameter

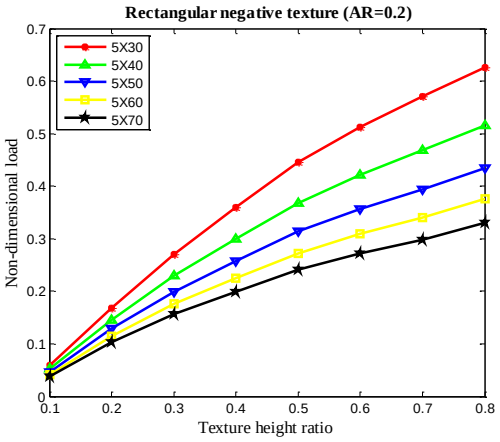

Fig 4.4.11: Non-dimensional load Vs. Texture height ratio for different distribution rectangle negative texture.

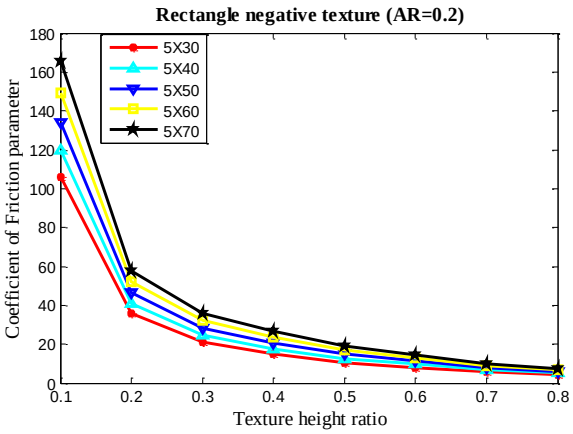

Fig 4.4.12: Coefficient of Friction parameter Vs. Texture height ratio for different distribution of negative rectangle texture.

From the figure 4.4.9 to 4.4.12 it shown the effect of aspect ratio and texture height ratio on non-dimensional load and co-efficient of friction parameter of rectangle negative texture .The non-dimensional load is found to be less in rectangle negative texture profile compared to

positive texture. It also shows coefficient of friction parameter is high compared to the positive texture.

4.5. Square Texture

4.5.1. Positive Asperity

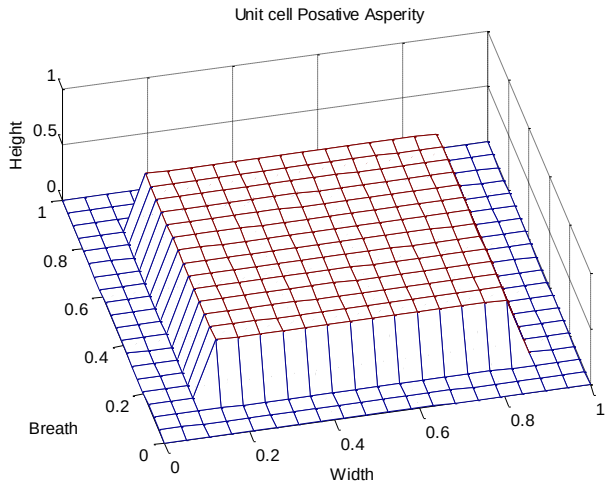

Fig 4.5.1: Single Positive Square Asperity

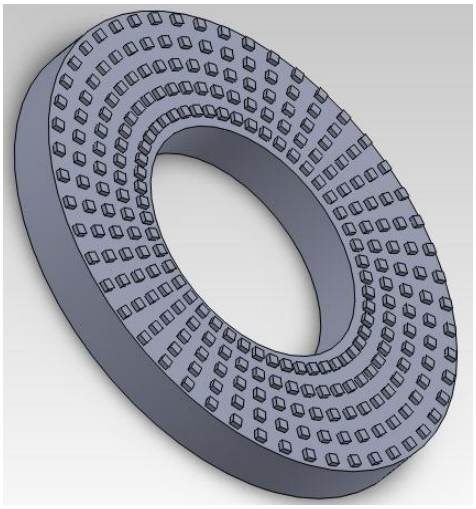

Fig 4.5.2: Distribution of Positive Square Asperities

Effect of Aspect Ratio on Non dimensional Load and Coefficient of Friction parameter

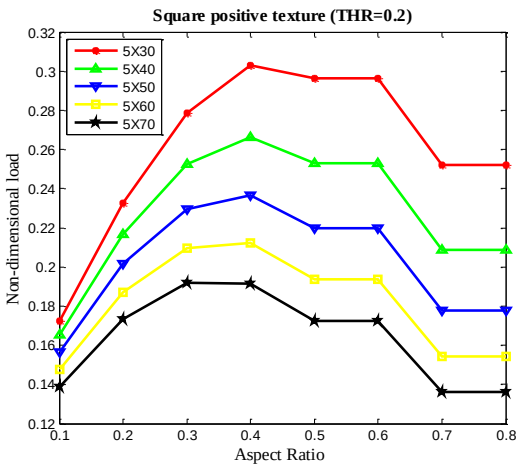

Fig 4.5.3: Non-dimensional load Vs. Aspect ratio for different distribution of positive square texture.

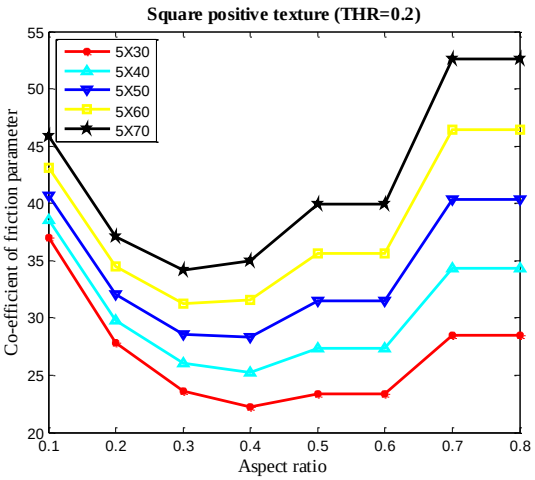

Fig 4.5.4: Coefficient of Friction parameter Vs. Aspect ratio for different distribution of positive square texture.

Effect of Texture Height Ratio on Non dimensional Load and Coefficient of Friction parameter

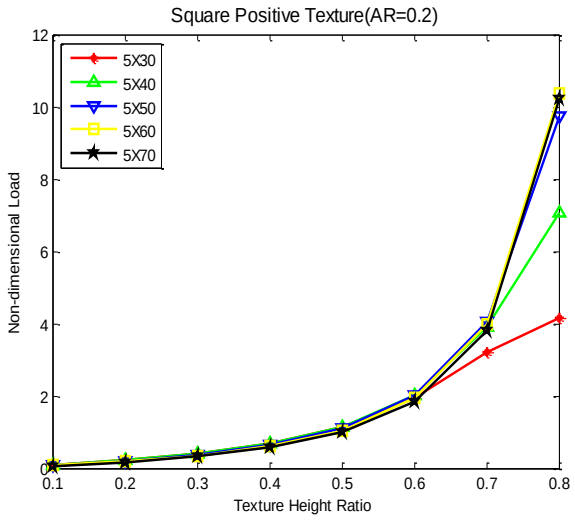

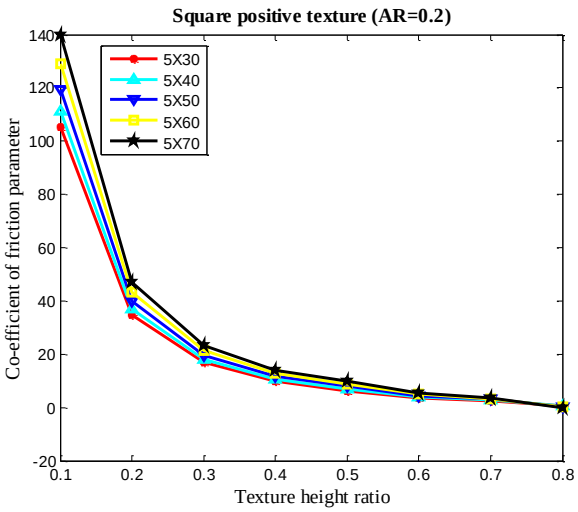

Fig 4.5.5:Non-Dimensional Load Vs. Texture height ratio for different distribution positive square texture.

Fig 4.5.6:Coefficient of Friction parameter Vs. Texture height ratio for different distribution of positive square texture.

Non-dimensional load and coefficient of friction parameter versus aspect ratio and texture height ratio are plotted in the figure from 4.5.3 to 4.5.6 .The non-dimensional load value is low and coefficient of Friction parameter value is high compared to rectangular positive texture profile

4.5.2. Negative Asperity

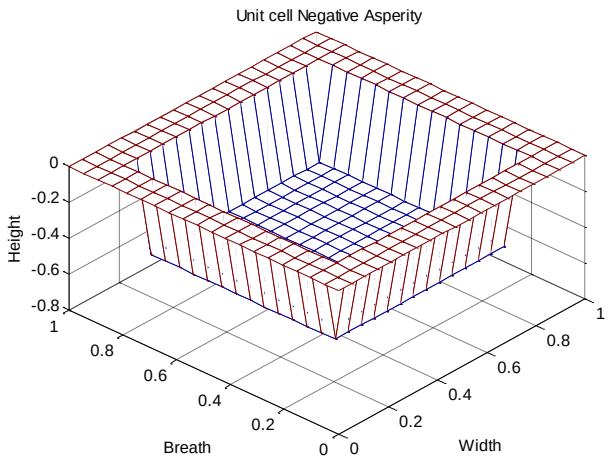

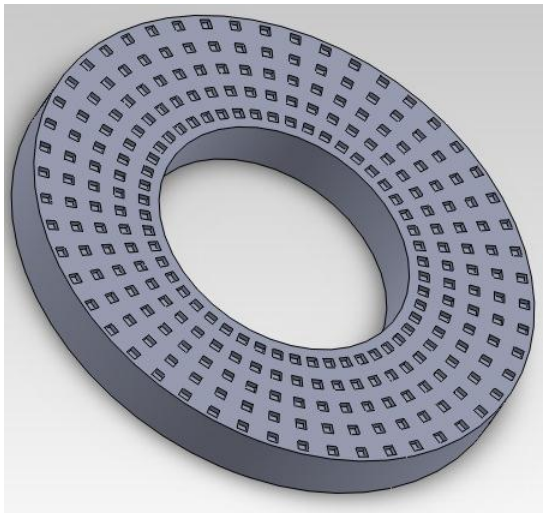

Fig 4.5.7: Single Negative Square Asperity

Fig 4.5.8: Distribution of Negative Square Asperities

Effect of Aspect Ratio on Non dimensional Load and Coefficient of Friction parameter

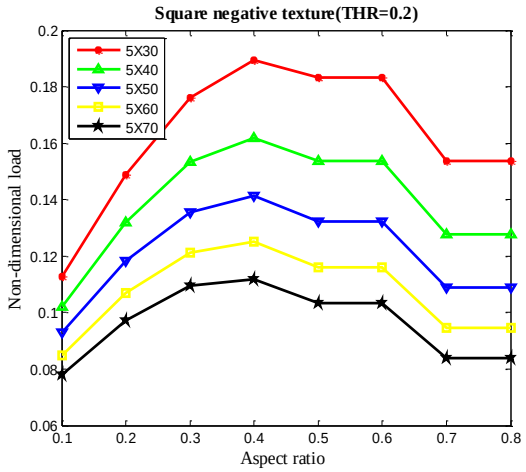

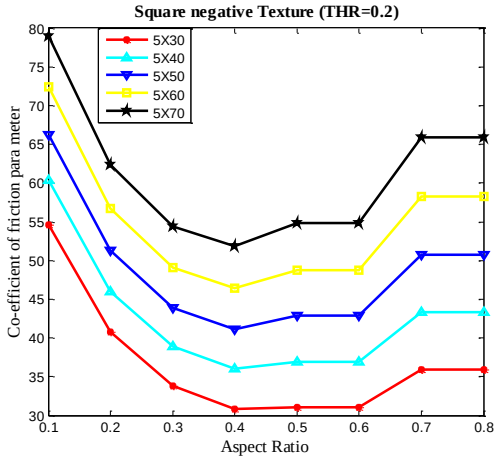

Fig 4.5.9:Non-Dimensional Load Vs. Aspect Ratio for different distribution of Negative Square Texture.

Fig 4.5.10: Coefficient of Friction parameter Vs. Aspect Ratio for different distribution of Negative Square Texture

Effect of Texture Height Ratio on Non-dimensional Load and Coefficient of Friction parameter

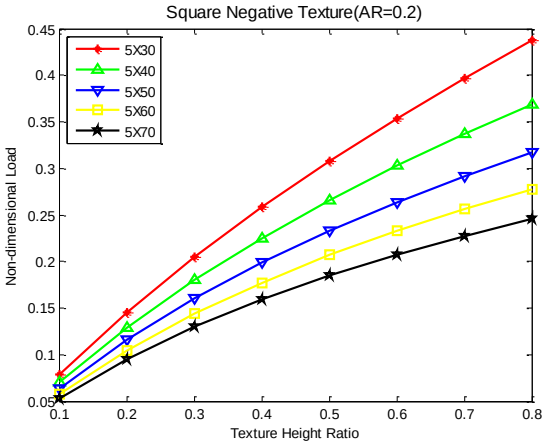

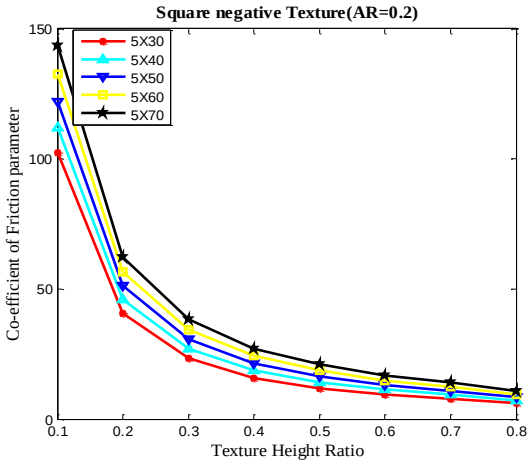

Fig 4.5.11: Non-Dimensional Load Vs. Texture height ratio for different distribution of negative square texture.

Fig 4.5.12: Coefficient friction parameter Vs. Texture height ratio for different distribution of negative square texture.

From figure 4.5.9 to 4.5.12, it shows the non-dimensional load is low comparable with positive square texture, but the coefficient friction parameters are very high for negative square structure.

A detail analysis on effect of type of texture profile, aspect ratio, and texture height ratio and texture density is summarized in table 4.1 and 4.2.

Sl.No	Unit shell	Type	No of texture	Maximum Non-dimensional Load and corresponding Aspect Ratio		Minimum Coefficient of Friction parameter and corresponding Aspect Ratio	
				Max.Non Dimension Load	Aspect Ratio	Min.Coefficient Of friction parameter	Aspect Ratio
1	Spherical	positive	5X30	0.21	0.5	32	0.5
		negative	5X30	0.15	0.5	41.5	0.5
2	Cylindrical	positive	5X30	0.26	0.4	26	0.4
		negative	5X30	0.17	0.4	36	0.4
3	Elliptical	positive	5X30	0.35	0.8	20	0.8
		negative	5X30	0.165	0.8	30	0.8
4	Rectangular	positive	5X30	0.4	0.6	17	0.6
		negative	5X30	0.23	0.6	25	0.6
5	Square	positive	5X30	0.3	0.4	23	0.4
		negative	5X30	0.19	0.4	31	0.4

Table 4.1: Aspect Ratio on Non Dimensional load and Coefficient of friction parameter

Sl.No	Unit shell	Type	No of texture	Maximum Non-dimensional Load and corresponding Texture Height ratio		Minimum Coefficient of Friction parameter and corresponding Texture Height Ratio	
				Max.Non-dimensional Load	Texture Height Ratio	Min.Coefficient Of friction parameter	Texture Height Ratio
1	Spherical	positive	5X30	2.6	0.8	9	0.8
		negative	5X30	0.47	0.7	18	0.8
2	Cylindrical	positive	5X30	6.5	0.8	2	0.8
		negative	5X30	0.41	0.6	17	0.8
3	Elliptical	positive	5X30	0.65	0.8	2	0.8
		negative	5X30	0.36	0.8	10	0.8
4	Rectangular	positive	5X30	18	0.8	0.01	0.8
		negative	5X30	0.63	0.8	10	0.8
5	Square	positive	5X30	4	0.8	0.01	0.8
		negative	5X30	0.44	0.8	8	0.8

Table 4.2: Texture height ratio on non-dimension load and coefficient of friction parameter.

5. Conclusion and Future Scope:

5.1 Conclusion

- Asperity shapes is less effective on coefficient of friction and non-dimension load however rectangular shapes shows better performance.
- Texture height ratio and aspect ratio plays an important role on controlling load and friction.
- The aspect ratio and texture height ratio to be maintained above 20% as there is better performance parameters beyond that point.
- Non dimensional load carrying capacity for positive asperity is higher than the negative asperity for most of the asperity type.
- Non dimensional load is increases as texture density decreases.
- Non dimensional load is increasing when texture height ratio is increased.
- Coefficient of friction parameter low in case of positive asperity.
- For most of the texture types non dimensional load is high when aspect ratio is in the range of 0.4-0.6 .
- Coefficient of friction parameter low when aspect ratio ranges 0.4-0.6.
- Coefficient of friction parameter is low when texture height ratio ranges from 0.7-0.8.

5.2 Future Scope

- Study on side flow of different texture profile bearing can be included along with load carrying capacity and Coefficient of friction.
- Orientation effect of different texture in the bearing.
- Texture distribution pattern in the bearing.
- Optimum values aspect ratio, texture height ratio and texture density to maximize performance parameter.

6. REFERENCES

[1] **Zhao, J., Sadeghi, F. and Nixon, H.**, "A Finite Element Analysis of Surface Pocket Effects in Hertzian Line Contact", ASME Journal of Tribology, vol. 122, pp. 47-54, 2000.

[2] **Tonder,** 'Hydrodynamic Effects of Tailored Inlet Roughnesses: Extended Theory", Tribology International, vol. 37, pp. 137-142, 2004.

[3] B**. Tower,** "First report on friction experiments" Proce.Inst. Mech. Engrs., London, vol.34, pp.632 -666, Nov-1883.

[4] **N. Petroff**, "Friction in machines and effect of lubrication", J.St. Peterburg, No.s 1,2,3,4, pp-71, 228,377 and 530, 1983.

[5] **O. Reynolds**, "On the theory of lubrication and its application and its application to Mr. B. Tower's experiments including experimental determination of viscosity of olive oil", phil.Trans Royal soc. London, vol.177, pp 157-234, 1886.

[6] D.B**. Hamilton**, J.A. Walowit, and C.M. Allen, "A theory of lubrication by micro asperities". ASME J Basic Engg. Vol.88, pp.177-185, 1966.

[7] **T. A. Osman**, M.Dorid, Z.S. Safar and M.O.A. Mokhatar, "Experimental Assessment of hydrostatic thrust bearing performance".Tribology International volume 29, Issue3, pp.233-239, 1996.

[8] **Marian Victor**, "Lubrication of textured surfaces", Universitaria report 2002 vol. 2. 2002.

[9] **Mircea D. Pascovici, Victor Marian, Daniel Gaman**., "Analytical and numerical approach of load carrying capacity for partially textured slider", International Nano tribology Conference Nano Sikkim II: Fiction and Biotribology, 2004.

[10] V G Marian, M Kilian, and W Scholz, "Theoretical and experimental analysis of a partially textured thrust pad bearing with square dimples" Proc. IMechE Vol. 221 Part J: J. Engineering tribology, 2007.

[11] **N Tala-Ighil, P Maspeyrot, M Fillon, and A Bounif,** ''Effects of surface texture on journal bearing characteristics under steady state operating conditions", Proc. IMechE Vol. 221 Part J: J. Engineering tribology, 2007.

[12] **Yu Haiwu , Wang Xiaolei and Fei Zhou,** "Geometric shape effects of surface texture on the generation of hydrodynamic pressure between conformal contacting surfaces", Tribology Letter, pp.123-130,2010.

[13] **jaw-ren** ,"Surface roughness effect on dynamic stiffness and damping characterstics of compensated hydrostatics thrust bearings",2000, 40 (2000) 1671–1689.

[14] **Xiaolei Wang, koji kota, koshi adachi, Kohz Aizawa**, Load carrying capacity map for the surface testure design of SiC thrust bearing sliding in water;2004,36(2003) 189-197.

[15] **T.S Luong, W.Potze , J.B Post , A .van Beek**,Numerical and experimental analysis of aerostatic thrust bearings with porous restrictors 2004;37(2004) 825-832.

[16] **Mohamed fourka, Marc Bonis,** "comparison between externally pressurized gas thrust bearing with different orifice and porous feeding systems",1997, 210 (1997) 311-317.

[17] **A.K Mishra,** Analysis of pneumatic instability of an aerostatic rectangular thrust bearing with an offset load,1987;122(1988) 1-12.

[18] **M.F Chen ,Y.T Lin**;static behavior and dynamic stabilityanalysis of groveed rectangular aerostatic thrust bearings by modified resistance network method,2001;35(2002) 329-338

[19] **I.Etsion**; Improving tribological performance of mechanical component by laser surface texturing;2004,vol-17,no-4.

[20] **Xiaolei Wang, Koshi Adachi**;Effect of texture shape on load carrying capacity of gas lubricated parallel slider bearing, Tribology International 36 (2003) 189–197.

[21] **W.U Ding-zhu,TAOJI-Zhong**;Analysis on the static performance of porous graphite aerostatic thrust bearings, Institute of Mechanical Manufacturing Technology, China Academy of Engineering Physics,Mianyang , China.

[22] **Y.Kligerman, A.Shinkarenko;**The effect of tapered edges on lubrication regima in surface texture elastomer seals,2011.

[23] **Mohamed Fourka, Yong Tian, Marc Bonis**;Prediction of stability of air thrust bearing by numerical analytical and experimental methods,1995,198(1996) 1-6.

[24] **Y.K Younes**, Dynamic load carrying capacities of a shell-shaped thrust bearing,1990;141(1991) 267-278.

[25] **S.N Rao**,Effect of slip flow in aerostatic porous rectangular thrust bearings,1979;61(1980) 77-86.